HHS Public Access

Author manuscript

Nature. Author manuscript; available in PMC 2019 October 10.

Published in final edited form as:

Nature. 2019 April ; 568(7752): 415–419. doi:10.1038/s41586-019-1101-y.

Associating HIV-1 envelope glycoprotein structures with states on the virus observed by smFRET.

Maolin Lu[1], **Xiaochu Ma**[1], **Luis R. Castillo-Menendez**[2,3], **Jason Gorman**[4], **Nirmin Alsahafi**[5,6], **Utz Ermel**[1], **Daniel S. Terry**[7], **Michael Chambers**[4], **Dongjun Peng**[4], **Baoshan Zhang**[4], **Tongqing Zhou**[4], **Nick Reichard**[1], **Kevin Wang**[1], **Jonathan R. Grover**[1], **Brennan P. Carman**[1], **Matthew R. Gardner**[8], **Ivana Nikic-Spiegel**[9], **Akihiro Sugawara**[10], **James Arthos**[11], **Edward A. Lemke**[12,13,14], **Amos B. Smith III**[10], **Michael Farzan**[8], **Cameron Abrams**[15], **James B. Munro**[16], **Adrian B. McDermott**[4], **Andrés Finzi**[5,6], **Peter D. Kwong**[4], **Scott C. Blanchard**[7,*], **Joseph G. Sodroski**[2,3,*], **Walther Mothes**[1,*]

[1]Department of Microbial Pathogenesis, Yale University School of Medicine, New Haven, CT, USA.

[2]Department of Cancer Immunology and Virology, Dana-Farber Cancer Institute, Boston, MA, USA.

[3]Department of Microbiology, Harvard Medical School, Boston, MA, USA.

[4]Vaccine Research Center, National Institute of Allergy and Infectious Diseases, National Institutes of Health, Bethesda, MD, USA.

[5]Department of Microbiology and Immunology, McGill University, Montreal, Quebec, Canada.

[6]Centre de Recherche du CHUM (CRCHUM), Département de Microbiologie, Infectiologie et Immunologie, Université de Montréal, Montreal, Quebec, Canada.

[7]Department of Physiology and Biophysics, Weill Cornell Medicine, New York, NY, USA.

[*]**Correspondence and requests for materials** should be addressed to S.C.B. or J.G.S. or W.M. scb2005@med.cornell.edu; Joseph_Sodroski@dfci.harvard.edu; walther.mothes@yale.edu.

Author contributions M.L., X.M., L.R.C.-M., N.A., J.G., J.B.M., A.F., P.D.K., S.C.B., J.G.S. and W.M. conceived these experiments. M.L., X.M., U.E., N.R., K.W., J.R.G., and B.P.C. performed mutagenesis, and M.L. and X.M. generated fluorescently labelled viruses. M.L., X.M. and D.S.T. performed labelling and smFRET imaging. M.L., X.M., S.C.B. and W.M. analysed the data. L.R.C.-M., J.G., M.C., N.A., A.F., D.P., B.Z., T.Z. and A.B.M. performed protein expression, purification and antibody-binding experiments. L.R.C.-M. performed negative-stain electron microscopy. J.B.M. and C.A. performed photophysical measurements and molecular dynamics simulations. A.S., J.A., A.B.S.III, I.N.-S., E.A.L., M.R.G. and M.F. provided reagents. M.L., P.D.K, S.C.B., J.G.S. and W.M. wrote the manuscript.

Competing interests S.C.B. holds an equity interest in Lumidyne Technologies. M.F. is a co-founder of Emmune, a company developing eCD4-Ig for clinical use. E.A.L. holds the patent WO 2012/104422 A1. S.C.B., J.B.M. and W.M. hold the patent US 959385324 B2.

Additional information

Extended data is available for this paper at https://doi.org/10.1038/s41586-019-1101-y.

Supplementary information is available for this paper at https://doi.org/10.1038/s41586-019-1101-y.

Reprints and permissions information is available at http://www.nature.com/reprints.

Publisher's note: Springer Nature remains neutral with regard to jurisdictional claims in published maps and institutional affiliations.

Online content

Any methods, additional references, Nature Research reporting summaries, source data, statements of data availability and associated accession codes are available at https://doi.org/10.1038/s41586-019-1101-y.

[8]Department of Immunology and Microbiology, The Scripps Research Institute, Jupiter, FL, USA.

[9]Werner Reichardt Centre for Integrative Neuroscience, University of Tuebingen, Tuebingen, Germany.

[10]Department of Chemistry, University of Pennsylvania, Philadelphia, PA, USA.

[11]Laboratory of Immunoregulation, National Institute of Allergy and Infectious Diseases, National Institutes of Health, Bethesda, MD, USA.

[12]Departments of Biology and Chemistry, Pharmacy and Geosciences, Johannes Gutenberg University Mainz, Mainz, Germany.

[13]Institute of Molecular Biology (IMB), Johannes Gutenberg University Mainz, Mainz, Germany.

[14]Structural and Computational Biology Unit and Cell Biology and Biophysics Unit, EMBL, Heidelberg, Germany.

[15]Department of Chemical and Biological Engineering, Drexel University, Philadelphia, PA, USA.

[16]Department of Molecular Biology and Microbiology, Tufts University School of Medicine, Boston, MA, USA.

Abstract

The HIV-1 envelope glycoprotein (Env) trimer mediates cell entry and is conformationally dynamic[1–8]. Imaging by single-molecule fluorescence resonance energy transfer (smFRET) has revealed that, on the surface of intact virions, mature pre-fusion Env transitions from a pre-triggered conformation (state 1) through a default intermediate conformation (state 2) to a conformation in which it is bound to three CD4 receptor molecules (state 3)[8–10]. It is currently unclear how these states relate to known structures. Breakthroughs in the structural characterization of the HIV-1 Env trimer have previously been achieved by generating soluble and proteolytically cleaved trimers of gp140 Env that are stabilized by a disulfide bond, an isoleucine-to-proline substitution at residue 559 and a truncation at residue 664 (SOSIP.664 trimers)[5,11–18]. Cryo-electron microscopy studies have been performed with C-terminally truncated Env of the HIV-1_{JR-FL} strain in complex with the antibody PGT15119. Both approaches have revealed similar structures for Env. Although these structures have been presumed to represent the pre-triggered state 1 of HIV-1 Env, this hypothesis has never directly been tested. Here we use smFRET to compare the conformational states of Env trimers used for structural studies with native Env on intact virus. We find that the constructs upon which extant high-resolution structures are based predominantly occupy downstream conformations that represent states 2 and 3. Therefore, the structure of the pretriggered state-1 conformation of viral Env that has been identified by smFRET and that is preferentially stabilized by many broadly neutralizing antibodies—and thus of interest for the design of immunogens—remains unknown.

To compare the conformational states of gp120 in Env trimers on the surface of virions of the BG505 subtype of HIV-1 (HIV-1_{BG505}) with gp120 in soluble gp140 SOSIP.664 trimers of HIV-1_{BG505} (hereafter, ‘BG505 sgp140 SOSIP.664’), we used enzymatic and non-natural amino acid strategies to site-specifically introduce donor and acceptor fluorophores in the variable regions V1 and V4 of gp120 at exactly the same positions (Extended Data Fig. 1a).

Positions in the HIV-1_{BG505} Env at which introduced tags do not disrupt Env processing and virus incorporation, infectivity or sensitivity to neutralization by trimer-specific antibodies have previously been identified[10]. Tags that were introduced at identical positions into BG505 sgp140 SOSIP.664 and DS-SOSIP.Mut4 (a further-stabilized variant of BG505 sgp140 SOSIP.664)[20] also had a negligible effect on antigenicity or the ability to assemble into compact trimers (Extended Data Fig. 1b, c). The tags enabled site-specific enzymatic incorporation of donor and acceptor fluorophores into gp120 on the surface of intact virus[8]. We prepared complete virus that carried—on average—one double-labelled HIV-1_{BG505} Env molecule per particle in the context of wild-type HIV-1_{BG505} Env[8] (Fig. 1a), and BG505 sgp140 SOSIP.664 trimers that carried—on average—one double-labelled protomer per trimer (Fig. 1b). Labelled viruses or trimers were immobilized within microfluidic sample chambers for total internal reflection smFRET imaging (Methods).

The observed anti-correlated relationship between donor and acceptor intensities, and resulting changes in FRET efficiency, were consistent with discrete motions of the V1 and V4 regions relative to each other within individual gp120 monomers (Fig. 1c, d). Histograms, comprised of smFRET data that were obtained from an ensemble of imaged virus, revealed three FRET states that were indicative of three major conformations of gp120 (Fig. 1e, f). Similar to Env from HIV-1_{JR-FL} and HIV-$1_{NL4–3}$ isolates[8], the native HIV-1_{BG505} Env predominantly occupied the low-FRET state 1 conformation (Fig. 1e). The native HIV-1_{BG505} Env spontaneously sampled both state 2 and state 3, which are characterized by high- and intermediate-FRET values, respectively (Extended Data Fig. 4c). By contrast, the BG505 sgp140 SOSIP.664 trimers—although they accessed three similar conformational states—predominantly occupied state 2 (Fig. 1f, Extended Data Fig. 4f). Similar results were observed for BG505 sgp140 DS-SOSIP.Mut4, and when using SOSIP.664 produced by a different laboratory (Fig. 1g, Extended Data Fig. 1c, d). Collectively, these data indicate that engineered sgp140 SOSIP.664 trimers are stabilized in conformations that more closely resemble the state 2 conformation than the state 1 conformation that predominates on intact virus particles.

Cryo-electron microscopy studies of mature HIV-1_{JR-FL} Env that lacks the cytoplasmic tail (HIV-1_{JR-FL} Env(ΔCT)), in complex with PGT151[19], (Extended Data Fig. 2a) have revealed a structure that is similar to that of the BG505 sgp140 SOSIP.664 trimer. We therefore used smFRET to examine the conformational state of HIV-1 Env bound to PGT151. The deletion of the cytoplasmic tail had little or no effect on the conformational landscape of Env (Extended Data Fig. 2b). However, PGT151 induced a notable shift in both HIV-1_{JR-FL} Env and HIV-1_{BG505} Env from a conformation similar to state 1 to a conformation similar to state 2 (Fig. 1h, Extended Data Fig. 2c–g). Similar results were obtained for variants of HIV-1_{JR-FL} Env and HIV-1_{BG505} Env that do not rely on the labelling tags (Extended Data Fig. 2h–l). In this case, fluorophores were ‘clicked’ onto unnatural amino acids that were introduced through the suppression of amber codons[21]. Thus, the gp120 conformations that are predominantly exhibited by both the BG505 sgp140 SOSIP.664 trimer and the PGT151-bound HIV-1_{JR-FL} Env differ from the predominant state-1 conformation of the virus-resident Env, and instead resemble state 2.

To understand the predominance of the state-2 conformation in BG505 sgp140 SOSIP.664, we introduced the SOSIP changes (that is, the disulfide bond and I559P substitution)—both separately and in combination—into the native HIV-1_{BG505} Env (Fig. 2a). Consistent with previous reports[22,23], both changes abrogated infectivity without altering Env processing or virus incorporation (Extended Data Fig. 3a, b). smFRET showed that, in combination, the changes stabilize a state- 2-like conformation in membrane-bound Env; this effect was largely due to the disulfide bond, both in HIV-1_{BG505} Env and in HIV-1_{JR-FL} Env (Fig. 2a, Extended Data Fig. 3c).

We next tested whether BG505 sgp140 SOSIP.664 retains the conformational plasticity of the native HIV-1_{BG505} Env in response to ligands specific to state 3 or state 1. Consistent with previous observations[10], the mature pre-triggered HIV-1_{BG505} Env transitioned into the state 3 conformation upon addition of soluble dodecameric CD4 (s$CD4_{D1D2}$–Igαtp (also called 12 × CD4), which consists of domains D1 and D2 of CD4 fused at the C-terminus to the immunoglobulin G (IgG) 1 heavy chain and immunoglobulin A secretory tailpiece) (Fig. 2b, Extended Data Fig. 3d, e, 1, 4c, d). The BG505 sgp140 SOSIP.664 similarly transitioned into a state-3-like conformation upon addition of s$CD4_{D1D2}$–Igαtp (Fig. 2c, Extended Data Fig. 4a, f, g). This observation is consistent with the large CD4-induced displacements between V1V2 and V4 that have previously been deduced from structural comparison of BG505 sgp140 SOSIP.664 and B41 sgp140 SOSIP.664 trimers in unliganded states, and in complex with monomeric soluble CD4[5,15]. By contrast, addition of the allosteric inhibitor BMS-378806 failed to re-equilibrate the conformational landscape of BG505 sgp140 SOSIP. 664 towards state 1, whereas this compound further stabilized the mature HIV-1_{BG505} Env in state 1 (Extended Data Fig. 3h, i, m). BG505 sgp140 SOSIP.664 was observed to exhibit a modest enrichment in a state-1-like conformation only upon addition of the more-potent analogue BMS-626529—at a 1,000-fold excess over its mean 95% inhibitory concentration (Fig. 2b, c, Extended Data Figs. 3j, k, n, 4b, e, h). These results indicate that state 1 is destabilized in BG505 sgp140 SOSIP.664, which probably explains why ligands specific to state 1—including both BMS inhibitors—have not been observed to stabilize the Env trimer in conformations that are distinct from the conformation that is observed in their absence[24].

Broadly neutralizing antibodies directed towards the V2 apex (PG16 and PGT145), the CD4-binding site (VRC01) and the glycan-V3 site (PGT122, PGT128 and 2G12)—as well as the entry inhibitor BMS-626529—have previously been observed to stabilize the Env of HIV-1_{NL4-3} and HIV-1_{JR-FL} virions in a state 1 conformation[8]. We tested additional broadly neutralizing antibodies (3BNC117 and 10–1074) that bind different epitopes on HIV-1_{BG505} (Extended Data Fig. 5a–c) and that suppress virus replication in animal models and in individuals infected with HIV-1[25–27]. The binding of 3BNC117, 10–1074 and PG9 to HIV-1 Env resulted in a dominant state 1 conformation (Fig. 3a–d, Extended Data Fig. 5d). By contrast, the non-neutralizing antibodies F105 and 17b induced a state 3 conformation (Extended Data Fig. 6).

We next tested the conformational preferences of antibodies elicited in cows[28] using the state-2-like immunogen, BG505 sgp140 SOSIP.664. Interestingly, each of the monoclonal antibodies (NC-Cow1, NC-Cow8, NC-Cow9 and NC-Cow10) isolated from immunized cows shifted the conformational landscape of HIV-1_{BG505} Env towards state 2 (Fig. 3e, f,

Extended Data Fig. 7a–h). Notably, the conformational landscape of HIV-1 Env bound by the NC-Cow9 antibody was indistinguishable from that of unliganded BG505 sgp140 SOSIP.664 (Fig. 3f). Thus, consistent with a state-2-like conformation of gp120, BG505 sgp140 SOSIP.664—as an immunogen in cows—elicits state-2-specific antibodies.

We next tested whether state 1 or state 2 can be detected using classic antibody staining of cell-expressed HIV-1 Env, followed by flow cytometry. HIV-1_{JR-FL} Env(ΔCT) that was pre-bound with BMS-626529, which stabilizes state 1, exhibited no decrease—or a slight increase—in the binding of PGT122 and 10–1074 antibodies, which prefer state 1 (Extended Data Fig. 7i). By contrast, pre-binding of ligands that prefer state 1 reduced the binding of the antibodies PGT151 and NC-Cow9, which are specific to state 2 (Extended Data Fig. 7i). Conversely, whereas the state-2-specific antibodies NC-Cow9 and PGT151 did not interfere with one another, the pre-binding of ligands specific to state 2 reduced the binding of ligands specific to state 1 (Extended Data Fig. 7j). Therefore, the distinct state 1 or state 2 preferences for Env by ligands can also be detected by conventional bulk measurements.

We considered the potential caveats of the tagging strategies and fluorophores used in the smFRET approach, but we did not observe evidence of abnormal dye behaviour or photophysical effects (Extended Data Fig. 8, Methods, Supplementary Table 1). Control experiments in which the positions of donor and acceptor fluorophores were reversed (Extended Data Fig. 8b–d) and fluorophores were attached via unnatural amino acids rather than peptide epitope tags also revealed nearly identical smFRET histograms (Extended Data Fig. 2h–l). We further validated the conclusions of the smFRET approach by assessing HIV-1 Env conformations and dynamics from a distinct structural perspective. Here we measured Env conformational dynamics using a click-labelled unnatural amino acid at residue 542 ($Arg542_{TAG}$) within gp41, in combination with the A1 enzymatic labelling tag in the gp120 V4 region (V4–A1) (Extended Data Fig. 9a). Compared with the VlV4-labelled HIV-1_{JR-FL} Env—in which the unliganded Env predominantly resides in a low-FRET conformation (Fig. 4a, b)—the unliganded HIV-1_{JR-FL} Env labelled in V4-A1 of gp120 and on $Arg542_{TAG}$ in the α6 helix of gp41 (α6-$Arg542_{TAG}$) largely exhibited a high-FRET state (Fig. 4c, d). The PGT151 ligand (which is specific to state 2) stabilized an intermediate-FRET state, and the 12 × CD4 ligand (which is specific to state 3) stabilized a low-FRET state in the V4-A1, α6- $Arg542_{TAG}$-labelled Env (Fig. 4c, d). The conformational landscape of Env again exhibited three distinct FRET states, each of which were sampled by the unliganded Env and differentially stabilized by PGT151 and 12×CD4. These findings lend further support to our conclusion that states 1, 2 and 3 correspond to three distinct conformations of the HIV-1 Env trimer (Fig. 4a–d).

We further monitored how HIV-1 Env is progressively activated by the potent bifunctional inhibitor eCD4-Ig(Q40A, mim2)[29]. HIV-1_{JR-FL} with the Env labelled at Asn136 in V1 and V4–A1 or with the Env labelled at $Arg542_{TAG}$ in α6 and V4-A1 was immobilized and continuously monitored over 60 min, after addition of eCD4-Ig(Q40A, mim2) (100 μg ml^{-1}) (Fig. 4e–j, Extended Data Fig. 9). Consolidating movies from 15-min intervals into FRET histograms (Fig. 4g, h) clearly revealed a time-dependent progression from state 1 through state 2 to state 3, independent of labelling strategy and structural perspective (Fig. 4i, j). These results confirm at the population level that—when activated synchronously—HIV-1

Env progressively transitions through the conformational states that have previously been identified as representing pre-triggered, default intermediate- and CD4-activated states of the Env trimer. Thus, the state 1 conformation of Env serves as a starting point for the temporal transitions that lead to downstream events related to membrane fusion.

These findings collectively suggest that extant high-resolution structures of the HIV-1 Env trimer closely resemble those of the state 2 intermediate, which is only transiently populated on the surface of native virus. The structure of pre-triggered state 1 remains unknown. Although state 2 is on a path to HIV-1 Env activation, state 1 is the predominant Env conformation that is found on the surface of most primary, and transmitted/founder HIV-1 isolates. Importantly, the structurally uncharacterized state 1 Env is a biologically relevant conformation that is preferentially bound by many broadly neutralizing antibodies. Evidence that the BG505 sgp140 SOSIP.664 proteins are in a conformation that is distinct from the native Env is also emerging from cross-linking studies[30]. These findings warrant focused initiatives to define the structure, molecular determinants and capacity of the state-1 conformation of Env to elicit broadly neutralizing antibodies.

METHODS

No statistical methods were used to predetermine sample size. The experiments were not randomized and investigators were not blinded to allocation during experiments and outcome assessment.

Preparation of tagged viruses

HIV-1_{BG505}, HIV-$1_{JR\text{-}FL}$ and HIV-$1_{nl4\text{–}3}$ viruses with Env that is double-tagged at V1–Q3 and V4–A1 were prepared for smFRET imaging, as previously described[8,10]. The double-tagged V1–Q3 V4–A1 Env carries a 6-amino acid Q3 tag in variable loop V1 and a 12-amino acid A1 tag in variable loop V4 (Q3, GQQQLG; Al, GDSLDMLEWSLM). HIV-1_{BG505}, HIV-$1_{JR\text{-}FL}$ and HIV-$1_{nl4\text{–}3}$ viruses with tagged Env were functionally validated before use[8,10]. For smFRET imaging, HIV-1 viruses were prepared as replication-incompetent particles that lack reverse transcriptase (ΔRT). A ratio 40:1 of wild-type gene:gene encoding the tagged Env was used to ensure that on average only one tagged protomer was available for imaging on a single virus particle[8,10]. Then, enzymatically tagged HIV-1_{BG505} virus was generated by co-transfecting HEK293 cells with a 40:1 ratio of wild-type full-length HIV-1_{BG505} Q23 ΔRT plasmid to Env tagged with V1–Q3 and V4–A1 HIV-1_{BG505} Q23 ΔRT plasmid (Extended Data Fig. 1a). HIV-$1_{JR\text{-}FL}$ viruses with a tagged Env were produced by pseudotyping a pNL4–3 ΔEnv (that is, lacking the gene for Env) ΔRT backbone with HIV-$1_{JR\text{-}FL}$ Env (Extended Data Fig. 2h, middle). A 40:1 plasmid ratio of Env expressing wild-type JR-FL gp160 pCAGGS and V1–Q3- and V4–Al-tagged JR-FL gp160 was co-transfected into HEK293 cells, along with the same amount of the pNL4–3 ΔEnv ΔRT plasmid. Double-tagged HIV-$1_{JR\text{-}FL}$ Env(ΔCT) was generated as above, with plasmids that encode JR-FL Env(ΔCT) and double-tagged JR-FL Env(ΔCT). Tagged HIV-1_{BG505} Env mutants that contain A501C and T605C (SOS), I559P or SOS and I559P, and HIV-$1_{JR\text{-}FL}$ SOS virus were prepared using the same ratio 40:1 of non-tagged Env SOS (or I559P, or SOS and I559P) to Env mutant SOS (or I559P, or SOS and I559P) and double-

tagged with V1-Q3 and V4–A1. Double-tagged full-length HIV-$1_{nl4–3}$ was made by co-transfecting HEK293 cells with a 40:1 ratio of wild-type, fulllength HIV-1 pNL4–3 ΔRT plasmid to double-tagged HIV-1 V1–Q3 and V4–A1 pNL4–3 ΔRT plasmid.

Labelled HIV-1_{BG505} and HIV-1_{JR-FL} viruses that carry dyes at single point substitutions (instead of enzymatic labelling peptides) were generated by suppression of amber (TAG) stop codons to introduce a clickable unnatural amino acid, followed by copper-free click chemistry to introduce the fluorophore[21]. Our system is based on an amber suppressor tRNA and the Y306A Y384F mutant of the *Methanosarcina mazei* pyrrolysine aminoacyl-tRNA-synthetase (PylRSAF) that accepts the clickable unnatural amino acid transcyclooct-2-ene lysine (TCO*, Sichem)[21]. In our laboratory, generation of HIV-1 viruses carrying Env with amber-suppressed clickable unnatural amino acids can be accomplished in one of three ways: (1) by using an engineered amberless full-length HIV-1_{BG505} Q23 genome that lacks all other TAG stop codons (a single TAG amber stop codon is introduced into Env of the full-length genome); (2) by using an expression plasmid for the gp160 of JR-FL (TAG introduced only into Env pcDNA3 expression plasmid) in combination with GagPol and long terminal repeat packaging plasmids; or (3) in combination with the amberless full-length HIV-1_{BG505} Q23 genome that lacks Env (ΔEnv). For example, HIV-1_{BG505} viruses labelled at $Ser401_{TAG}$ in V4 and V1–Q3 (Extended Data Fig. 2h, bottom), which carry the clickable unnatural amino acid TCO* at position $Ser401_{TAG}$ in V4 and the Q3 tag in V1, were produced by transfecting an engineered amberless full-length HIV-1_{BG505} Q23 ΔRT genome, an Env mutant that carries a single amber codon at position $Ser401_{TAG}$, and a bi-cistronic plasmid that carries the amber suppressor tRNA and PylRSAF (1/3 of the amount of the plasmid that encodes the gene for Env). The unnatural amino acid TCO* was added to the amber suppression transfection system at 250 μM. Clickable HIV-1_{JR-FL} virus (V1–$Asn136_{TAG}$ V4–A1) was produced by transfecting an amberless Q23 backbone ΔEnv ΔRT and a JR-FL Env mutant that carries a single amber codon at position $Asn136_{TAG}$ in V1 and the A1 tag in V4 (Extended Data Fig. 2h). HIV-1_{JR-FL} virus V4-A1 α6-$Arg542_{TAG}$ (Extended Data Fig. 9a) was produced by transfecting an amberless Q23 backbone ΔEnv ΔRT and a JR-FL Env mutant that carries the A1 tag in the gp120 V4 loop and an amber in position Arg542 in the α6 helix of gp41, respectively.

Tagged viruses were collected 40 h after transfection, filtered and concentrated by centrifugation over a 15% sucrose cushion at 25,000 r.p.m. (SW28, Beckman Coulter) for 2 h and resuspended in labelling buffer (50 mM pH 7.5 HEPES, 10 mM $MgCl_2$, 10 mM $CaCl_2$).

Preparation and validation of tagged BG505 sgp140 SOSIP.664

Positions in native HIV-1_{BG505} Env at which the enzymatic labelling peptides (Q3, GQQQLG; A1, GDSLDMLEWSLM) are tolerated in the respective V1 and V4 variable regions of gp120 without affecting Env expression, processing, virus incorporation and virus infectivity have previously been identified[10]. The short Q3 and A1 peptides were then introduced at identical positions into V1 and V4 (V1–Q3 and V4–A1) of BG505 sgp140 SOSIP.664 or DS-SOSIP.Mut4[20] (Extended Data Fig. 1a). For purification and

immobilization for total internal reflection fluorescence microscopy, the BG505 sgp140 SOSIP.664 also carried a D7324 affinity tag[11].

The BG505 sgp140 SOSIP.664 trimers were produced by transfection of HEK293 Freestyle (293F) cells with plasmids that encode the respective proteins, and the protein was purified from the serum-free culture supernatant. To generate double-tagged BG505 sgp140 SOSIP. 664, we chose plasmid transfection conditions that favour an excess of trimers that carry only one double-labelled protomer over trimers that contain two or three double-labelled protomers. In brief, assuming random assembly into a trimer, the number of V1V4-tagged BG505 sgp140 SOSIP.664 protomers in a trimer follows a binomial distribution. In the case of the ratio of 20:1 of wild-type to V1V4-tagged protomers, statistics predict that 86.38% of the BG505 sgp140 SOSIP.664 trimer remains untagged, 12.96% contains only a single double-tagged protomer, 0.65% has two double-tagged protomers and 0.01% contains all protomers tagged. Among tagged BG505 sgp140 SOSIP.664 trimeric proteins, more than 95% contain only a single double-tagged gp120, with the remaining two gp120 subunits in the trimer being wild type. As only the fluorescently labelled protein will be seen by total internal reflection fluorescence microscopy, this procedure guarantees that the vast majority of Env trimers that we studied carry a single double-labelled gp120 subunit.

BG505 sgp140 SOSIP.664 in the presence of a plasmid that expresses furin. In brief, 100% BG505 sgp140 SOSIP.664 and 100% V1V4-tagged BG505 sgp140 SOSIP.664 were generated by transfecting only one of the plasmids, together with a plasmid that expresses furin. Subsequently, 36 h after transfection, cells were removed from the serum-free supernatant by centrifugation at 6,000g. The Env trimers in the supernatant were then purified by affinity chromatography using a 2G12 antibody (Polymun Scientific), which was coupled to CNBr Sepharose 4B beads (GE Healthcare). Bound Env trimers were eluted with 3 M MgCl2 and diluted immediately in 20 mM Tris, 100 mM NaCl, pH 8.0. The sample was concentrated and further purified by size-exclusion chromatography in 100 mM phosphate, 100 mM NaCl, pH 7.4 buffer using a Superose 6 10/30 column (GE Healthcare). Peaks that corresponded to trimeric fractions were collected and used for the experiments.

The immunogenic and structural features of the 20:1 and 100% tagged BG505 sgp140 SOSIP.664 proteins were evaluated using enzyme-linked immunosorbent assay (ELISA) and electron microscopy (Extended Data Fig. 1b). In brief, 96-well plates were coated with a panel of anti-Env antibodies overnight at room temperature, then washed and blocked with 5% BSA. Plates were further incubated with BG505 sgp140 SOSIP.664 trimers for 1 h at 37 °C, followed by extensive washing and incubation with a rabbit anti-gp120 HRP polyclonal antibody (Abcam) for 1 h at 37 °C. HRP signal was measured using a Western Lighting oxidizing and luminol reagent (Perkin Elmer Life Sciences). Light emission was measured with a Mithras LB 940 luminometer. Each ELISA was repeated at least six times, and averaged.

We further evaluated the trimeric structures using negative-staining electron microscopy. The purified 20:1 tagged BG505 sgp140 SOSIP.664 trimers (5 μl at 100 μg/ml) were adsorbed to a glow-discharged carbon-film grid, stained with 2% uranyl acetate and imaged on an FEI Tecnai F20 transmission electron microscope with a 4,000 × 4,000 CCD camera (80 keV,

50,000× magnification, 40 electrons per Ångstrom^2). Approximately 20,000 particles were selected from the micrographs and assembled into class averages using common-lines methods in EMAN2.1[31], in a reference-free manner. C3 symmetry was imposed during the reconstruction/refinement.

In addition to the BG505 sgp140 SOSIP.664 trimers prepared in the Sodroski laboratory, two tagged BG505 sgp140 SOSIP.664 trimers were generated and purified in the Kwong laboratory. In the latter case, the 20:1 wild-type to V1V4-tagged BG505 sgp140 SOSIP.664 proteins were generated similarly to the method described above, but molecules that expose the V3 loop were negatively selected using an anti-V3 antibody cocktail as previously described[18]. In addition, the stabilized sgp140 SOSIP.664 variant (DS-SOSIP.Mut4) was purified as previously described[20]. Both purified protein preparations were assessed using Meso Scale Discovery electrochemiluminescence immunoassay (Extended Data Fig. 1c). In brief, 96-well Multi-Array MSD plates (catalogue number L15XA-3) were coated with a panel of HIV-1 neutralizing antibodies: CD4-induced (17 and 48b, with and without sCD4), CD4 binding site (VRC01, VRC03, b12 and F105), V2 apex-directed antibodies (PGT145 and VRC26.25), glycan V3 site-directed antibodies (2G12, PGT121 and PGT128) and weakly neutralizing V3-directed antibodies (447–52D, 3074 and 2557, with and without soluble CD4), gp41-gp120 interface antibodies (PGT151, 35O22, 8ANC195 and VRC34.01) and a negative control antibody CR9114 (an influenza virus antibody that does not recognize HIV-1 Env) in duplicate (30 μl per well) at an antibody concentration of 4 μg/ml in PBS buffer. The plates were incubated overnight at 4 °C. The next day, the plates were washed (0.05% Tween 20 in PBS) and blocked with 150 μl blocking buffer (5% MSD blocker A, catalogue number R93BA-4; MSD) for 1 h on a vibrational shaker at 650 r.p.m. at room temperature. Where indicated, 1 μM sCD4 was added to BG505 sgp140 SOSIP.664 trimers, before they were added to the MSD plate. Both BG505 sgp140 DS-SOSIP.664 and sgp140 DS-SOSIP.Mut4 trimers were titrated in serial twofold dilutions, starting from 5.0 μg/ml. The serially diluted trimers were then transferred (25 μl/well) to the MSD plates above, and incubated for 2 h with shaking at 650 r.p.m. at room temperature. After the plates were washed several times, 2G12 and Sulfo-Tag (catalogue number R91AO-1; MSD) at 2 μg/ml were added to the plates (25 μl per well), and further incubated for 1 h with shaking as above. After the washing step, the plates were read using read buffer (catalogue number R92TC-1; MSD) on an MSD Sector Imager 2400.

Preparation of fluorescently labelled viruses and BG505 sgp140 SOSIP.664 trimers

The Q3 and A1 double-tagged viruses and BG505 sgp140 SOSIP.664 trimers allowed the incorporation of Cy3B (Cy3B(3S)-cadaverine) and Cy5 (Cy5(M3)-CoA; LD650-CoA) for the real-time observation of relative movements of V1 and V4 in the gp120 subunit of an individual trimer using smFRET[8,10,14]. For labelling, the sucrose-purified tagged viruses were resuspended in 50 mM HEPES buffer (pH 7.5, 10 mM $MgCl_2$ and 10 mM $CaCl_2$) containing Cy3B(3S)-cadaverine (0.5 μM), transglutaminase[32] (0.65 μM; Sigma Aldrich), LD650-CoA (0.5 μM) (Lumidyne Technologies) and AcpS[33] (5 μM, Abcam) and incubated at room temperature. In Extended Data Fig. 8b–d, Cy3B(3S)-CoA and Cy5(M3)-cadaverine were used instead of Cy3B(3S)-cadaverine and Cy5(M3)-CoA. For click labelling, Env variants that carry TCO* were clicked using H-tetrazine conjugates of Cy3 or Cy5

(Lumidyne Technologies). PEG2000-biotin (Avanti Polar Lipids) was added to the labelling reaction at a final concentration 0.02 mg/ml, and incubated for an additional 30 min before the virus was purified by ultracentrifugation at 40,000 r.p.m. (SW41, Beckman Coulter) over a 6–18% Optiprep (Sigma Aldrich) gradient. The biotin-lipid facilitates the immobilization of the samples on the streptavidin-coated microfluidic sample chambers.

BG505 sgp140 SOSIP.664 proteins with a 20:1 ratio of wild-type:V1V4-tagged gp120 were enzymatically labelled with donor and acceptor fluorophores in the labelling buffer described above, at 37 °C for 48 h, and purified away from free dye using Zeba spin desalting columns (Thermo Fisher). For the immobilization on passivated streptavidin-coated microfluidic imaging chambers, the BG505 sgp140 SOSIP.664 protein was incubated with the anti-HIV-1 gp120 D7324 antibody (Aalto Bio Reagents) at 4 °C overnight followed by a 2-h incubation on ice with the secondary biotinylated rabbit anti-sheep IgG (H+L) antibody (Thermo Fisher).

smFRET data acquisition and analysis

All smFRET imaging was acquired on a in-house-built total internal reflection fluorescence microscope, as described[8,34]. Microfluidic imaging chambers passivated with a mixture of PEG and biotin-PEG were coated with streptavidin (Invitrogen). Fluorescently labelled virions and BG505 sgp140 SOSIP.664 proteins were then immobilized on passivated streptavidin-coated microfluidic imaging chambers. Donor fluorophores were excited by the evanescent field generated by total internal reflection of a 532-nm diode-pumped solid-state laser (Opus, Laser Quantum). Donor and acceptor fluorescence was collected through a 60 × 1.27-NA water-immersion objective (Nikon), spectrally split by a MultiCam-LS device (Cairn) with a dichroic filter (Chroma), and recorded by two synchronized ORCA-Flash4.0v2 sCMOS cameras (Hamamatsu). Movies were recorded at 25 frames per second for 80 s, using custom software implemented in LabView (National Instruments). All smFRET imaging was performed in buffer containing 50 mM Tris (pH 7.4), 50 mM NaCl, a cocktail of triplet-state quenchers[35] and 2 mM protocatechuic acid (PCA) with 8 nM protocatechuic-3,4-dioxygenase (PCD) to remove molecular oxygen[36]. Under ligand- and antibody-binding conditions, all of the ligand and antibody concentrations were ~5-fold above the 95% inhibitory concentration unless indicated otherwise. Where indicated, fluorescently labelled virus and/or BG505 SOSIP.664 trimers were pre-incubated with 10 μg/ml PGT151, 10 μg/ml sCD4D1D2-Igatp, 100 μM inhibitors (BMS-378806 and BMS-626529), 50 μg/ml broadly neutralizing antibodies (bNAbs) (3BNC117, PG9 or 10–1074, NIH AIDS Reagents Program), 100 μg/ml non-neutralizing antibodies (17b or F105) for 30 min at room temperature before imaging.

All data analysis was performed using the customized MATLAB (Mathworks) program SPARTAN[34]. The background signal was identified at the fluorophore bleaching point and subtracted from the fluorescence signal. Donor and acceptor fluorescence intensity trajectories were extracted from movies, and used to calculate FRET efficiency according to FRET = $I_a/(\gamma I_d + I_a)$, in which $\mathbf{I}d$ and $I\mathbf{a}$ are the fluorescence intensities of donor and acceptor, respectively, and γ is the correlation coefficient, correcting for the difference in detection efficiencies of the donor and acceptor channels. FRET trajectories identified on the

basis of the criteria of sufficient S:N ratio, anti-correlated features between donor and acceptor intensity, single dye photobleaching and fluorescence lifetime were compiled into FRET histograms. Only one protomer carrying two dyes within one trimer on one virion (1-protomer:1-trimer:1-virion) that showed clear anti-correlated features of donor and acceptor fluorescence and single fluorescence bleaching point met our criteria. A single bleaching point was used to filter out rarely observed multiple donors and acceptors or even the rare aggregates. The FRET histograms were fit to the sum of three Gaussian distributions (with means and variances, Extended Data Table 1) in MATLAB on the basis of the observation of original FRET signals and hidden Markov modelling[8,10]. We used hidden Markov modelling to fit the data with a three-state Markov model that gave a smaller log-likelihood value than a two-state Markov model. Fitting the data into a four-state model did not lower the log-likelihood value. Therefore, at present, a three-state Markov model provides the simplest explanation of the data. For signals obtained from the Env of different HIV-1 strains, and viruses with different tags, the shapes of Gaussian distributions vary slightly. Therefore, the mean of each FRET state was determined for each labelled virus separately (Extended Data Table 1). The occupancy of each state was determined by the area under each Gaussian distribution (Extended Data Table 1). Transition density plots (Extended Data Fig. 4), which display the relative frequency of state-to-state transitions, were idealized using a segmental k-means algorithm[37].

Besides the observations of the same three conformational states from two different structural perspectives (Fig. 4), several other observations support the existence of the state 1 conformation of Env. First, the low-FRET value of V1V4-labelled Env represents a defined conformational state that is clearly separated from background, as evidenced by discrete photobleaching events[8,10] (Fig. 1c, d, 2a, 3a, c, e, Extended Data Fig. 4a, b). Second, the occupancy of state 1 changes in response to biologically relevant Env ligands (as described here and in previous studies[8,10]). Third, the low-FRET state is not simply a consequence of non-specific fluorophore interactions with Env or viral membranes, as neither fluorophore associated with virus preparations in the absence of enzymatic labelling tags[8,10]. Dyes in the V1 and/or V4 positions for single- or double-labelled virus, or BG505 sgp140 SOSIP.664, exhibit fluorescence lifetimes that are similar to those of free dyes (Supplementary Table 1). Moreover, molecular dynamics simulations performed for the loops, enzymatic labelling tags, linkers and dyes using known structures revealed that the V1 and V4 positions are distal to the viral membrane (Extended Data Fig. 8a). Fourth, reversing the positions of donor and acceptor fluorophores on the virus revealed nearly identical smFRET histograms for the unliganded Env, as well as similar responses to ligands (Extended Data Fig. 8b–d). Fifth, the predominance of state 1 for the unliganded Env and the stabilization of state 2 in the presence of PGT151 were reproduced when V1 and V4 peptide epitope tags were replaced with labelled unnatural amino acids (Extended Data Fig. 2h–l).

Molecular dynamics simulations

Atomic coordinates for the BG505 sgp140 SOSIP.664 trimer were obtained from the Protein Data Bank (accession code 4ZMJ). Coordinates for the Q3 and A1 peptides, and for the missing amino acids in the V4 loop, were generated in PyMol (Schrodinger), and inserted into one gp120 domain in the 4ZMJ BG505 sgp140 SOSIP model, using LEaP in the

AmberTools software package. The modified BG505 sgp140 SOSIP trimer was charge-neutralized, and solvated in explicit water using the TIP3P solvent model with periodic boundary conditions in LEaP. The protein was parameterized with the amber force field (ff14SB). The system was then energy-minimized and equilibrated in the NPT ensemble, using NAMD version 2.12.

Atomic coordinates for the Cy3B and Cy5 fluorophores and linkers were generated in PyMol. The geometry of the fluorophores was first optimized at the AM1 level of theory, using the sqm program in AmberTools. Further geometry optimization and electrostatic potential calculations were then performed at the 'HF/6–31G(d)' level of theory in Gaussian 9 (Gaussian). Partial atomic charges were then determined by restrained electrostatic potential fitting in antechamber in AmberTools. Atom types and force-field parameters were taken from the generalized amber force field (GAFF2). The fluorophores and linkers were then bound to the Q3 and A1 peptides in the BG505 sgp140 SOSIP.664 model using LEaP. Three unique starting positions for each fluorophore were generated by randomizing the torsion angles of the fluorophore linkers. Again, the systems were charge-neutralized and solvated, and minimized and equilibrated in the NPT ensemble. Only the V1 and V4 loops, the Q3 and A1 peptides, the linkers, the fluorophores and the solvent were allowed to move; the positions of all core SOS and I559P trimer atoms were fixed. Temperature and pressure were maintained at 300 K and 1 atm, using Langevin dynamics and the Nose-Hoover Langevin piston method, respectively. Subsequently, 50-ns simulations were run using NAMD on the Stampede2 machine at the Texas Advanced Computing Center.

Infectivity and titration measurements

The infectivity of HIV-1_{BG505} or HIV-1_{JR-FL} with wild-type or mutant Env that carries SOS, I559P or SOS and I559P mutations—or amber-suppressed Env—was determined using a vector containing an HIV-1 long terminal repeat that expresses a Gaussia luciferase reporter[8,38]. In brief, HIV-1_{BG505} viruses that carry wild-type or mutant Env were generated by transfecting 60–80% confluent HEK293 cells with full-length HIV-1_{BG505} Q23[39] and an intron-regulated luciferase reporter plasmid (HIV-1-InGluc) at a ratio of 6:1 using Fugene 6 (Promega). Transfection of HIV-1_{BG505} or HIV-1_{JR-FL} with Env that carries amber TAG codons included plasmids that encode the amber suppressor tRNA and PylRSAF (1/3 of the amount of the plasmid carrying the gene for Env) and 250 μm TCO*. Culture supernatant was collected 40 h after transfection, filtered through a 0.45-μm filter (Pall) and titred on TZMbl cells. Gaussia luciferase activity was measured at 48 h after infection using a Gaussia luciferase substrate (NEB). Neutralization assays were conducted by incubating viruses with ligands or antibodies at the indicated concentrations for 30 min at room temperature, before addition to TZMbl cells. The level of infection relative to that seen in the absence of ligand or antibody is reported.

Flow cytometry

The binding preferences of ligands and antibodies for Env conformational states of wild-type HIV-1_{JR-FL} Env(ΔCT) were assessed by flow cytometric analysis. Antibody combinations (first pre-bound + second probe) (Extended Data Fig. 7i, j) with known Env binding-site competition were not included into the analysis. In our experiments, 3×10^5

HEK293T cells were transfected by the calcium phosphate method with the HIV-1JR-FL Env(ΔCT)-expressing plasmid along with a pIRES-GFP vector, at a ratio of 2 μg of pcDNA3.1 HIV-1_{JR-FL} Env(ΔCT) to 0.5 μg of GFP-expressing plasmid. Then, 16 h after transfection, cells were washed with fresh medium (DMEM) and epitope exposure was evaluated 24 h later. Alternatively, transfected HEK293T cells were incubated for 1 h at room temperature with increasing concentrations of first-pre-bound BMS-529 (0–200 μM) before detection with second-probe anti-HIV-1 Env monoclonal antibodies (1 μg/ml PGT122, 10–1074, 3BNC117, PGT151 and NC-Cow9 antibody isolated from BG505 sgp140 SOSIP.664-immunized cows) that were conjugated using cyanine-based far-red fluorescence dye (Mix-n-Stain CF-647 Antibody labelling kit, Sigma). The largely conformation-independent anti-gp120 outer domain 2G12 antibody was used to monitor Env expression on the cell surface. For antibody competition assays, transfected cells were incubated with increasing concentrations of first-pre-bound anti-HIV-1 Env monoclonal antibodies 3BNC117, 10.1074, PGT122, PGT151 and NC-Cow9 (0, 1, 5 or 10 μg/ml) for 1 h at room temperature, followed by a 30-min incubation at room temperature with second-probe anti-HIV-1 Env antibodies coupled to C-F 647. Antibody binding was detected by gating on GFP-positive cells with an LSRII cytometer (BD Biosciences). Data analysis was performed using FlowJo v.X.0.7 (Tree Star). Mean fluorescence intensity, indicating the level of second-probe binding, was normalized to that seen in the absence of first-pre-bound ligand. Data are from experiments that were repeated at least five independent times, and averaged.

Reporting summary

Further information on research design is available in the Nature Research Reporting Summary linked to this paper.

Data availability

The data that support the findings of this study are available from the corresponding authors upon reasonable request.

Code availability

The full source code of SPARTAN[34], which was used for all analysis of smFRET data, is available at http://www.scottblanchardlab.com/software.

Extended Data

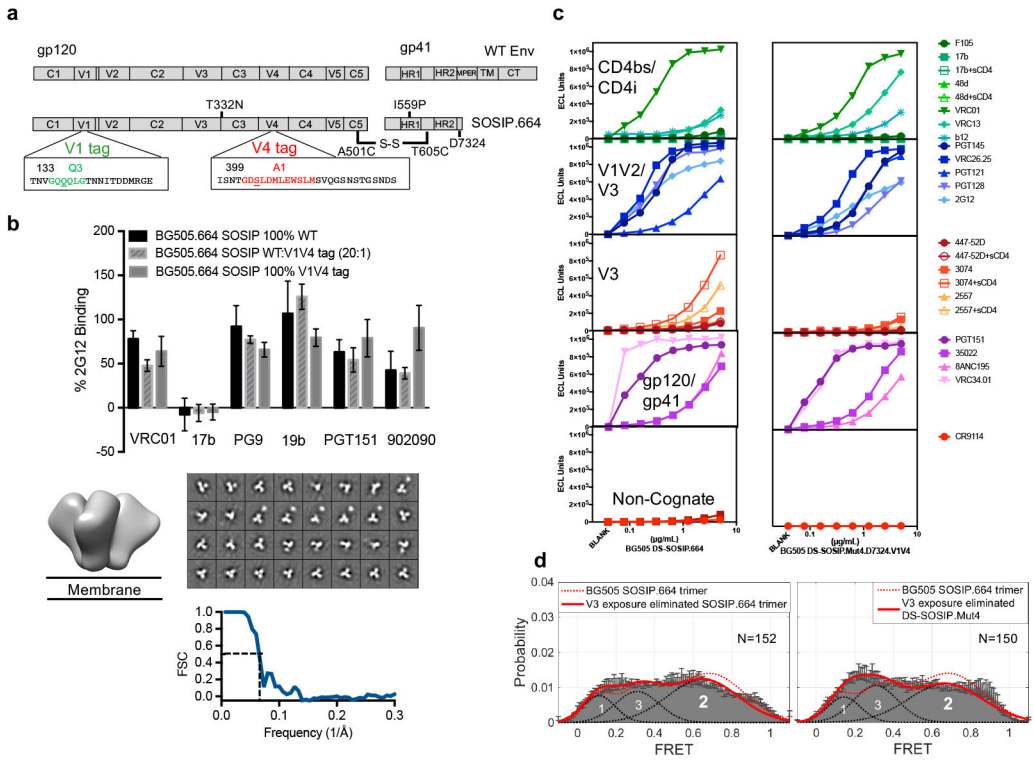

Extended Data Fig. 1 |. Tagged BG505 sgp140 SOSIP.664 proteins largely retain their known immunogenic features and preferentially sample state-2-like conformations.

a, Schematics for wild-type (WT) BG505 Env and BG505 sgp140 SOSIP.664 with D7324 affinity tag; V1–Q3 peptide in green, V4–A1 peptide in red. **b**, Validation of tagged BG505 sgp140 SOSIP.664. Top, antigenic profile of 100% untagged (WT), 100% double-tagged V1V4 (V1–Q3 V4–A1), and 20:1 of untagged to double-tagged BG505 sgp140 SOSIP.664. Binding by the indicated VRC01, 17b, PG9, 19b, PGT151 and 902090 antibodies was assessed from two independent ELISA assays in hexaplets and displayed as percentage of 2G12 binding (mean ± s.d.). The epitope for the antibody 902090 was more exposed in the 100%-tagged BG505 sgp140 SOSIP.664 than in the untagged BG505 sgp140 SOSIP.664, although this was not the case for the 1:20 tagged:wild-type trimers used for our smFRET analyses. The insertion of the Q3 tag into all three V1 regions of Env may exert local effects on the V2 β-barrel that contains the 902090 epitope (residues 171–177). Bottom, reference-free negative-staining electron microscopy two-dimensional class averages with representative trimeric density map of the BG505 sgp140 SOSIP.664 (wild type:V1V4-tagged at a 20:1 ratio) used for smFRET imaging. A Fourier shell correlation is also provided. **c**, Antigenic characteristics of BG505 sgp140 DS-SOSIP.664 (left) and 100% V1V4-tagged BG505 DS-SOSIP.Mut4 (right), determined by MSD. Antibodies are labelled. CD4bs, CD4 binding site; CD4i, CD4-induced; V1V2, V1V2-directed; V3, V3 glycan site-directed; gp120/gp41, interface between gp120 and gp41. Antigenic profiles of BG505 dS-SOSIP.664 (left) and 100% V1V4-tagged DS-SOSIP.Mut4 (right) after V3-negative selection were assessed by a panel of CD4-induced antibodies (17 and 48b, with and without sCD4), CD4 binding site antibodies (VRC01, VRC03, b12 and weakly neutralizing F105), V1V2-directed antibodies (PGT145 and VRC26.25), V3 glycan site-directed antibodies

(2G12, PGT121, PGT128) and weakly neutralizing V3-directed antibodies (447–52D, 3074 and 2557, with and without soluble CD4), gp41–gp120 interface antibodies (PGT151, 35O22, 8ANC195 and VRC34.01) and the negative-control antibody CR9114 (an influenza virus antibody that does not recognize HIV-1 Env). ECL, electrochemiluminescence. **d**, The indicated BG505 sgp140 SOSIP.664 variants exhibit predominantly state-2-like conformations. FRET histograms for V1V4-tagged BG505 sgp140 SOSIP.664 with molecules after V3-negative selection (left), and for the stabilized BG505 sgp140 SOSIP.664 variant DS-SOSIP.Mut4[20] (right) (see Methods). Histograms represent mean ± s.e.m., determined from three independent populations of smFRET traces.

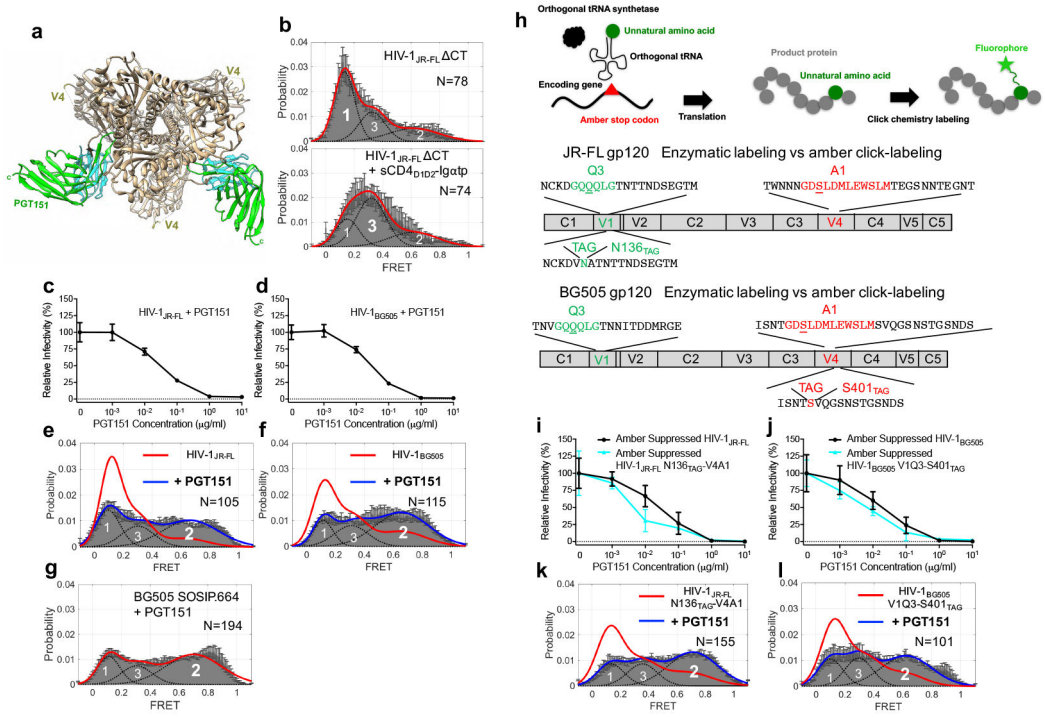

Extended Data Fig. 2 |. Binding of PGT151 stabilizes a state-2-like conformational state of HIV-1 Env.

a, Structure of HIV-1_{JR-FL} Env(ΔCT) in complex with PGT151[19]. Two PGT151 antigen-binding fragments are distant from the positions of the gp120 variable loops (V1 and V4) that carry the fluorophores. **b**, Population FRET histograms of unliganded HIV-1_{JR-FL} Env(ΔCT), and HIV-1_{JR-FL} Env(ΔCT) in the presence of 10 μg ml^{-1} $sCD4_{D1D2}$–Igαtp. **c**–**f**, Addition of PGT151 at neutralizing concentrations (10 μg ml^{-1}) shifts the conformational landscapes for enzymatically labelled HIV-1_{JR-FL} (**c**, **e**) and HIV-1_{BG505} (**d**, **f**) from the unliganded preference towards state 1 (red solid lines) to a preference for state 2 (blue solid lines). **g**, The addition of PGT151 to BG505 sgp140 SOSIP.664 did not alter the dominance of the state-2-like conformation exhibited in the absence of PGT151. **h**, Schematic of use of amber-suppressor tRNAs to introduce unnatural amino acids that can be clicked with fluorophores (**h**, top; see Methods), and schematic comparison between the Q3 and A1 double tag used for enzymatically labelling and click-labelling of V1 and V4 of HIV-1_{JR-FL} (**h**, middle) and HIV-1_{BG505} Env (**h**, bottom). To introduce the unnatural amino acid TCO*, Asn136 in the V1 loop of HIV-1_{JR-FL} or Ser401 in the V4 loop of HIV-1_{BG505} was genetically altered to an amber (TAG) stop codon. **i**–**l**, Experiment as in **c**–**f**, characterizing the conformational landscape upon binding of PGT151 to click-labelled HIV-1_{JR-FL} V1–$Asn136_{TAG}$ V4–A1 (**i**, **k**), and HIV-1_{BG505} V1–Q3 V4–$Ser401_{TAG}$ (**j**, **l**). Neutralization data (mean ± s.d.) are averaged from three independent experiments in triplicates (**c**, **d**, **i**, **j**). FRET population histograms represent mean ± s.e.m., determined from three independent populations of smFRET traces.

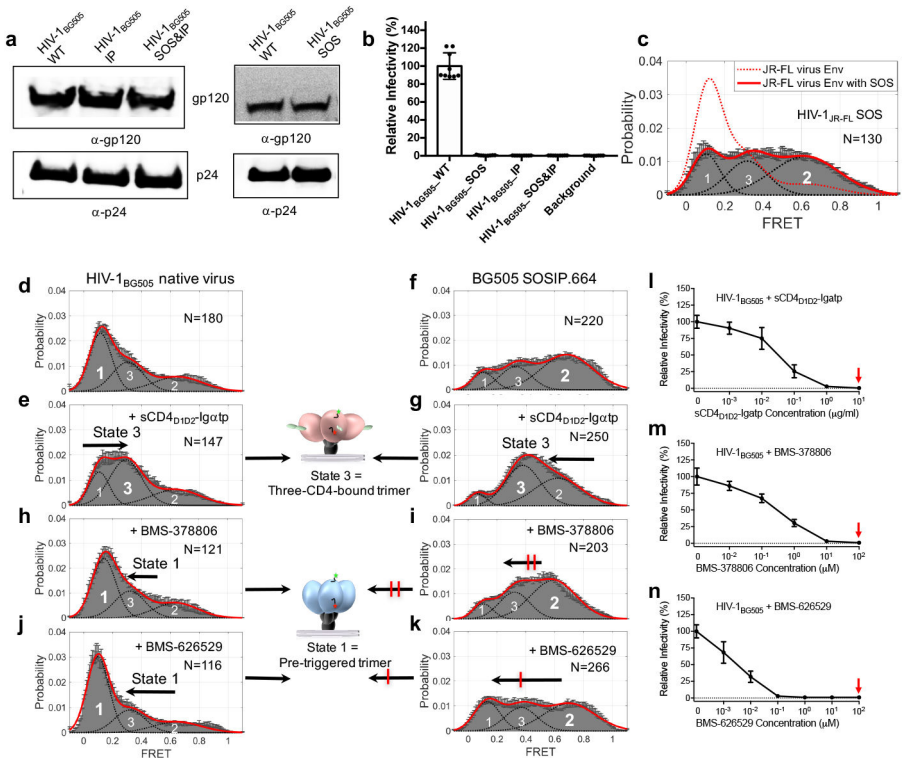

Extended Data Fig. 3 |. SOS and I559P effects on infectivity and conformational plasticity of sgp140 SOSIP.664.

a, SOS and/or I559P (IP) changes introduced into native HIV-1_{BG505} Q23 Env do not influence Env processing or virus incorporation. Env expression, processing and virus incorporation for HIV-1_{BG505} Q23 carrying SOS, I559P and SOS and I559P (SOS&IP) changes were tested by centrifugation of viruses from cell culture supernatants, followed by sodium dodecyl sulfate-polyacrylamide gel electrophoresis in the presence of dithiothreitol, and western blotting using the antiserum to HIV-1 gp120 (NIH AIDS reagent no. 288) and HIV-1 p24 monoclonal antibody (NIH AIDS reagent no. 3537). Experiments were repeated twice. **b**, The structure-stabilizing modifications A501C and T605C (SOS) and I559P used in the design of BG505 sgp140 SOSIP.664 abort HIV-1 infectivity. Infectivity of HIV-1_{BG505} Q23 SOS and I559P was measured by a Gaussia Luciferase assay, and normalized to that of wild-type HIV-1_{BG505} Q23. **c**, FRET histogram of HIV-1_{JR-FL} Env carrying SOS, confirming similar data for HIV-1_{BG505} Env that the SOS change is largely responsible for the state 2 stabilization of Env on virus. **d**, **e**, FRET histograms of HIV-1_{BG505} Env in the absence (unliganded, **d**) or the presence of sCD4_{D1D2}–Igαtp (**e**). **f**, **g**, Experiments as in **d**, **e** for BG505 sgp140 SOSIP.664. **h**–**k**, FRET histograms of HIV-1_{BG505} Env and BG505 sgp140 SOSIP.664 in the presence of the entry inhibitors BMS-378806 (**h**, **i**) and BMS-626529 (**j**, **k**). **l**–**m**, Neutralization of HIV-1_{BG505} by sCD4_{D1D2}–Igαtp (**l**), BMS-378806 (**m**) and BMS-626529 (**n**). Red arrows indicate concentrations used in smFRET experiments. Histograms correspond to those in the main figures: in **d** (Fig. 1e), **e** (Fig. 2b, top), **f** (Fig. 1f), **g** (Fig. 2c, top), **j** (Fig. 2b, bottom) and **k** (Fig. 2c, bottom). Infectivity and neutralization curves represent mean ± s.d. from three replicates in

triplicates. FRET population histograms represent mean ± s.e.m., determined from three independent populations of smFRET traces.

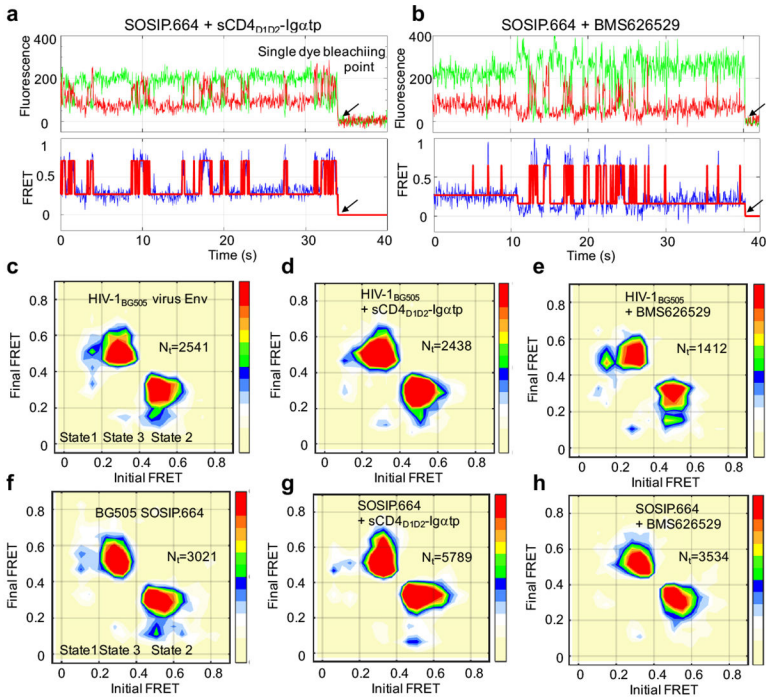

Extended Data Fig. 4 |. Conformational remodelling of HIV-1_{BG505} and BG505 sgp140 SOSIP.664 by $sCD4_{D1D2}$–Igαtp and BMS-626529.

a, **b**, Examples of fluorescence traces of BG505 sgp140 SOSIP.664 in the presence of 10 μg ml^{-1} $sCD4_{D1D2}$–Igαtp (**a**), and 100 μM BMS-626529 (**b**). Arrows indicate single-step photobleaching events that define the background of our smFRET assay. **c**–**e**, Transition density plots of HIV-1_{BG505} in the absence (**c**) or presence (**d**) of $sCD4_{D1D2}$–Igαtp, or in the presence of BMS-626529 (**e**). Transition density plots that indicate the relative frequency of state-to-state transitions were generated from individual traces (180 traces in Fig. 1e, 147 traces in Fig. 2b (top), and 116 traces in Fig. 2b (bottom)). n, number of total transitions observed. **f**–**h**, Transition density plots of BG505 sgp140 SOSIP.664 under the same experimental conditions as those shown in **c**–**e.**

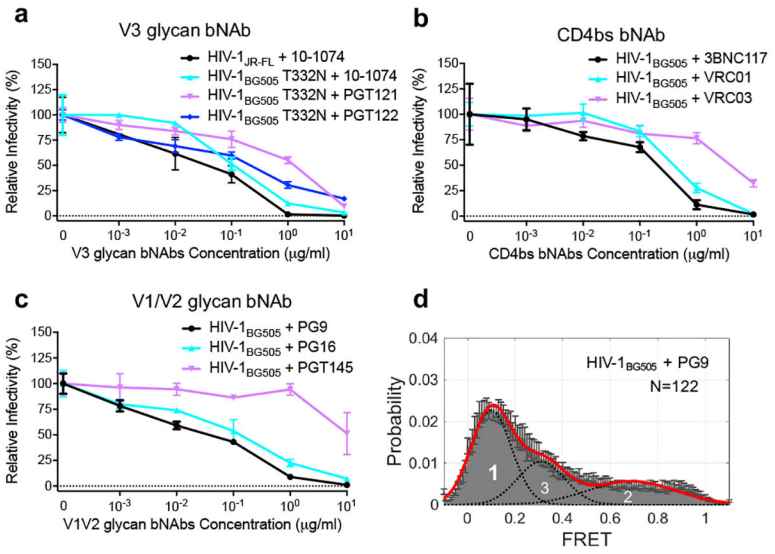

Extended Data Fig. 5 |. Many bNAbs neutralize and exhibit preference for the state 1 conformation of HIV-1.

a–**c**, Neutralization of native HIV-1_{BG505} by bNAbs that recognize different Env epitopes: V3 glycan site-directed bNAbs 10–1074, PGT121 and PGT122 (**a**); CD4 binding site bNAbs 3BNC117, VRC01 and VRC03 (**b**); and V1V2 glycan bNAbs PG9, PG16 and PGT145 (**c**). Only bNAbs that potently neutralize HIV-1_{BG505} or HIV-1_{JR-FL} and allowed smFRET imaging at an antibody concentration 5 times above the 95% inhibitory concentration were analysed further (Fig. 3b, d). Neutralization data (mean ± s.d.) were averaged from three independent experiments in triplicate. **d**, FRET histogram that shows that HIV-1_{BG505} Env remains in state 1 in the presence of PG9 (50 μg ml^{-1}). FRET population histograms represent mean ± s.e.m., determined from three independent populations of smFRET traces.

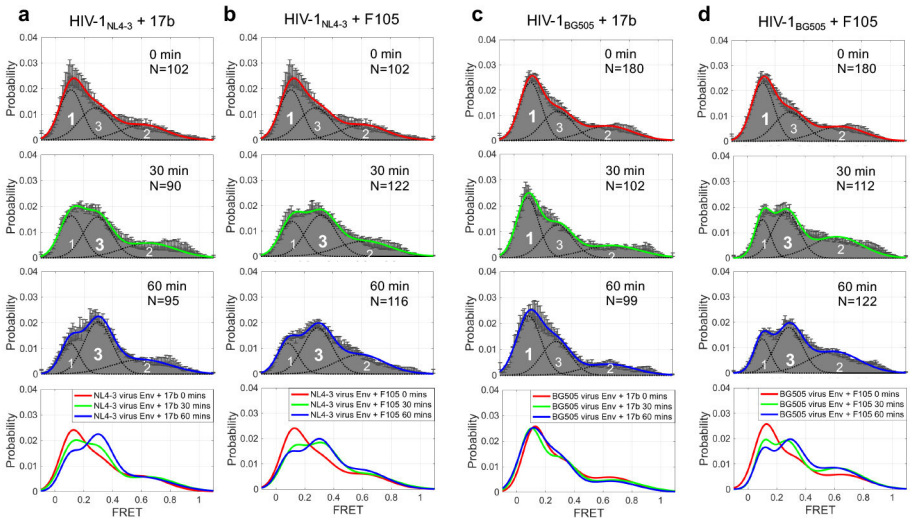

Extended Data Fig. 6 |. Conformational preferences of non-neutralizing antibodies for HIV-1 Env on virus.

a, **b**, FRET histograms and overlaid landscapes of HIV-$1_{NL4–3}$ in the presence of 100 μg ml $^{-1}$ 17b (**a**) and 100 μg ml^{-1} F105 (**b**) acquired after 0 min, 30 min and 60 min of incubation. **c**, **d**, FRET histograms and overlaid landscapes of HIV-1_{BG505} in the presence of 17b (**c**) and F105 (**d**), acquired after 0 min, 30 min and 60 min of incubation. Non-neutralizing antibodies have preference for the state 3 conformation of Env. Note that in contrast to the tier 1 HIV-1 isolate NL4–3, the tier 2 isolate BG505 does not respond to 17b. FRET population histograms represent mean ± s.e.m., determined from three independent groups of smFRET traces.

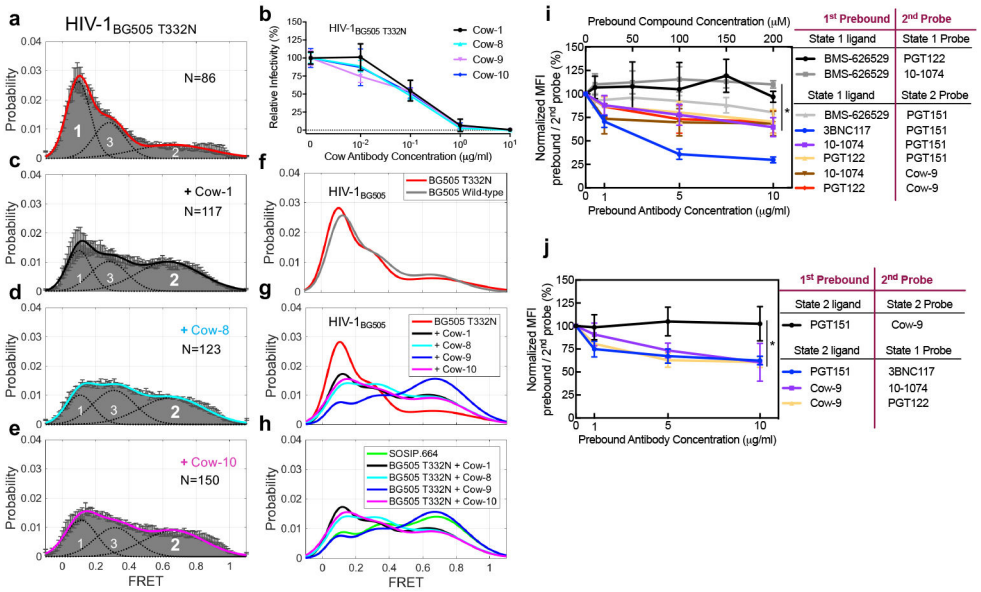

Extended Data Fig. 7 |. Antibodies isolated from cows immunized using BG505 sgp140 SOSIP.664 immunogens exhibit a preference for state 2.

a, FRET histogram of HIV-1_{BG505}(T332N). **b**, Neutralization curves of HIV-1_{BG505} by NC-Cow1, NC-Cow8, NC-Cow9 and NC-Cow10 antibodies. Data are presented as mean ± s.d. determined from three independent experiments in triplicate. **c**–**e**, FRET histograms of native HIV-1_{BG505} in the presence of 10 μg ml^{-1} NC-Cow1 (**c**), NC-Cow8 (**d**) and NC-Cow10 (**e**). **f**, The FRET histogram of HIV-1_{BG505} that carries the T332N substitution in Env is overlaid with that of wild-type HIV-1_{BG505}. The T332N substitution in HIV-1_{BG505} Env does not detectably change the conformation of the Env. **g**, **h**, Cow antibodies (NC-Cow1, NC-Cow8, NC-Cow9 and NC-Cow10) shift the conformational landscape of native Env on the virus from state 1 towards that of BG505 sgp140 SOSIP.664 (state 2). FRET population histograms (**a**, **c**–**e**) represent mean ± s.e.m., from three independent populations of smFRET traces. **i**, **j**, Ligand preferences for states 1 and 2 probed by antibody staining of cell-expressed HIV-1_{JR-FL} Env(ΔCT). Increasing amounts of the first ligand were pre-bound to cells for 1 h. The cells were washed, incubated with the second dye-labelled probe for 30 min, and the binding was quantified by flow cytometry. The ratio of measured mean fluorescence intensity (MFI) was normalized to that seen in the absence of pre-bound ligand (Methods). Matched combinations (state 1 and state 1 or state 2 and state 2) and non-matched combinations (state 1 and state 2 or state 2 and state 1) at the highest concentration of pre-bound first ligand were compared, and statistical significance was evaluated using a paired Student's two-sided *t*-test. $*P < 0.05$. Note that the strong interference between 3BNC117 and PGT151 is due to a steric clash between the two antibodies, and was included as a control.

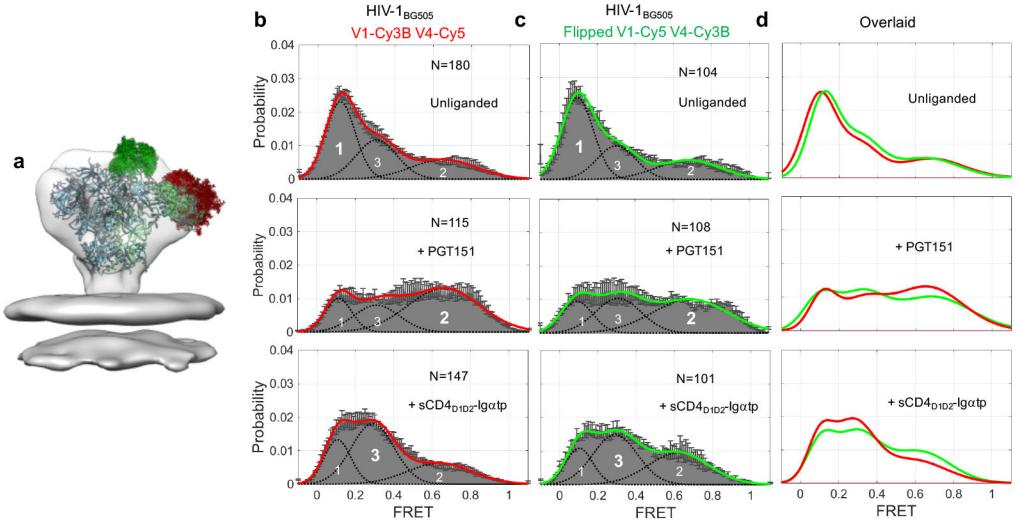

Extended Data Fig. 8 |. Validating the behaviour of dyes used for smFRET.

a, The 50-ns molecular dynamics simulations of fluorophore tumbling on the BG505 sgp140 SOSIP.664 trimer (4ZMJ) shows that dyes in V1 and V4 are far from the viral membrane. Molecular dynamics simulation was performed to account for movements of loops, enzymatic labelling tags, linkers and dyes to describe the possible dye tumbling space within 50 ns. The sampled space was docked into the approximately 20 Á structure of the HIV-1 virus Env spike determined by cryo-electron tomography[4]. A 50-ns molecular dynamics simulation is not temporally comparable to the time resolution of single-molecule imaging at 40 ms, or the timescale of observed conformational changes of Env (milliseconds to seconds). **b**–**d**, Conformational properties of the HIV-1_{BG505} Env remain highly similar when the dyes are flipped. **b**, Reference FRET histograms of HIV-1_{BG505} that carries Cy3B in V1 and Cy5 in V4, in unliganded form (from Fig. 1e), in the presence of PGT151 (from Fig. 1h) or in the presence of $sCD4_{D1D2}$–Igαtp (from Fig. 2b). **c**, FRET histograms of HIV-1_{BG505} Env that carries Cy5 in V1 and Cy3B in V4 (see Methods), in the absence and in the presence of 10 μg ml^{-1} PGT151 or 10 μg ml^{-1} $sCD4_{D1D2}$–Igαtp, respectively. **d**, Overlaid conformational landscapes of HIV-1_{BG505} Env labelled as in **c** with flipped dyes (green), compared to HIV-1_{BG505} Env labelled as in **b** (red). FRET population histograms represent mean ± s.e.m., determined from three independent populations of smFRET traces.

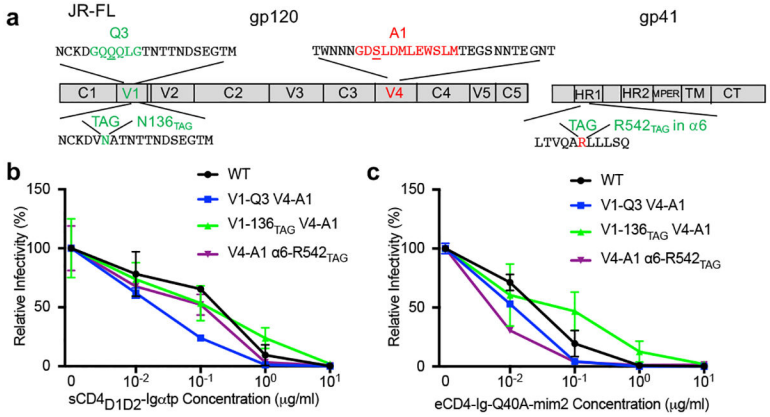

Extended Data Fig. 9 |. Suppressed HIV-1_{JR-FL} that carries amber positions in gp120 and gp41 enables smFRET imaging of Env from two distinct perspectives.

a, Schematic of tagged sites in HIV-1_{JR-FL} Env that were used for enzymatic labelling and amber stop codon (TAG)-suppressed incorporation of unnatural amino acids for click labelling. HIV-1_{JR-FL} V1–Q3 V4–A1 carries the Q3 peptide in the V1 loop and the A1 peptide in the V4 loop. HIV-1 $_{JR-FL}$ V1–Asn136$_{TAG}$ V4–A1 carries a TAG at position Asn136 in V1 and the A1 peptide in V4. HIV-1_{JR-FL} V4–A1 α6-Arg542$_{TAG}$ carries the A1 tag in gp120 V4 and a TAG at Arg542 in the α6 helix of gp41. **b**, **c**, Neutralization of HIV-1_{JR-FL} wild type, 100%-peptide-tagged V1–Q3 V4–A1, 100%-amber-suppressed V1–Asn136$_{TAG}$ V4–A1 and V4–A1 α6-Arg542$_{TAG}$ by sCD4$_{D1D2}$–Igαtp (**b**), and eCD4-Ig(Q40A, mim2) (**c**). Neutralization curves (**b**, **c**) represent mean ± s.d. from three replicates in triplicates

Extended Data Table 1 |

Relative occupancies and determining parameters in each of three observed FRET states

HIV-1$_{BG505}$	Curve fitting R-squared	State 1	State 2	State 3
		μ: 0.1+/-0.03	μ: 0.65+/-0.05	μ: 0.33+/-0.04
		σ: 0.07+/-0.01	σ: 0.17+/-0.03	σ: 0.10+/-0.02
Unliganded	0.9949	45% +/- 6%	24% +/- 5%	31% +/- 8%
+ PGT151	0.9573	17% +/- 8%	60% +/- 11%	23% +/- 15%
+ sCD4$_{D1D2}$-Igαtp	0.9860	20% +/- 8%	30% +/- 11%	50% +/- 13%
+ BMS-378806	0.9933	50% +/- 13%	22% +/- 7%	28% +/- 7%
+ BMS-626529	0.9796	58% +/- 8%	18% +/- 11%	24% +/- 14%
+ 3BNC117	0.9915	52% +/- 9%	23% +/- 9%	25% +/- 12%
+ PG9	0.9760	49% +/- 4%	25% +/- 6%	26% +/- 4%
+ 17b	0.9903	48% +/- 4%	19% +/- 6%	33% +/- 14%
+ F105	0.9754	20%+/-4%	38%+/-10%	42% +/- 6%
SOS & IP unliganded	0.9755	25% +/- 6%	49% +/- 7%	26% +/- 10%
SOS unliganded	0.9553	23% +/- 12%	54% +/- 15%	23% +/- 11%
IP unliganded	0.9604	40% +/- 12%	30% +/- 8%	29% +/- 15%
T332N Unliganded	0.9844	46% +/- 7%	26% +/- 8%	28% +/- 10%
+ Cow 1	0.9788	25% +/- 8%	47% +/- 7%	28% +/- 12%
+ Cow 8	0.9887	21% +/- 7%	44% +/- 8%	35% +/- 12%
+ Cow 9	0.9758	8% +/- 4%	68% +/- 6%	24% +/- 8%
+ Cow 10	0.9700	29% +/- 9%	41% +/- 5%	30% +/- 12%
Flipped dyes unliganded	0.9780	50% +/- 11%	24% +/- 7%	26% +/- 13%
+ PGT151	0.9338	20% +/- 4%	49% +/- 7%	31% +/- 6%
+ sCD4$_{D1D2}$-Igαtp	0.9877	19% +/- 7%	37% +/- 8%	44% +/- 12%
HIV-1$_{BG505}$ V1Q3-S401$_{TAG}$	Curve fitting R-squared	**State 1**	**State 2**	**State 3**
		μ: 0.11+/-0.01	μ: 0.61+/-0.01	μ: 0.30+/-0.02
		σ: 0.07+/-0.01	σ: 0.17+/-0.03	σ: 0.10+/-0.02
unliganded	0.9940	53% +/- 9%	18% +/- 11%	29% +/- 14%
+ PGT151	0.9387	23% +/- 13%	51% +/- 9%	26% +/- 15%
BG505 SOSIP.664	Curve fitting R-squared	**State 1**	**State 2**	**State 3**
		μ: 0.1+/-0.03	μ: 0.65+/-0.05	μ: 0.33+/-0.04
		σ: 0.07+/-0.01	σ: 0.17+/-0.03	σ: 0.10+/-0.02
Unliganded	0.9737	13% +/- 6%	62% +/- 4%	25% +/- 7%
+ PGT151	0.9056	22% +/- 13%	58% +/- 10%	20% +/- 15%
+ sCD4$_{D1D2}$-Igαtp	0.9973	7% +/- 1%	44% +/- 1%	49% +/- 12%
+ BMS-378806	0.9860	10% +/- 4%	61% +/- 10%	29% +/- 11%
+ BMS-626529	0.9676	26% +/- 7%	48% +/- 8%	26% +/- 10%
V3 exposure eliminated	0.9201	16% +/- 10%	58% +/- 11%	26% +/- 10%
DS-SOSIP.Mut4	0.9254	16% +/- 10%	54% +/- 9%	31% +/- 12%

HIV-1$_{JR-FL}$	Curve fitting R-squared	State 1	State 2	State 3
		μ: 0.1+/-0.03	μ: 0.65+/-0.04	μ: 0.30+/-0.03
		σ: 0.07+/-0.01	σ: 0.17+/-0.03	σ: 0.10+/-0.02
Unliganded	0.9821	53% +/- 11%	19% +/- 6%	28% +/- 13%
+ PGT151	0.9434	29% +/- 11%	49% +/- 10%	22% +/- 12%
+ sCD4$_{D1D2}$-Igαtp	0.9726	24% +/- 10%	27% +/- 14%	49% +/- 15%
+ 10-1074	0.9884	60% +/- 10%	20% +/- 7%	20% +/- 5%
SOS unliganded	0.9836	23% +/- 4%	50% +/- 8%	27% +/- 8%
ΔCT unliganded	0.9776	50% +/- 9%	23% +/- 13%	27% +/- 14%
+ sCD4$_{D1D2}$-Igαtp	0.9712	23% +/- 13%	25% +/- 10%	52% +/- 12%
HIV-1$_{JR-FL}$ N136$_{TAG}$-V4A1	Curve fitting R-squared	**State 1**	**State 2**	**State 3**
		μ: 0.12+/-0.02	μ: 0.75+/-0.05	μ: 0.35+/-0.03
		σ: 0.07+/-0.01	σ: 0.17+/-0.03	σ: 0.10+/-0.02
unliganded	0.9809	52% +/- 12%	20% +/- 14%	28% +/- 10%
+ PGT151	0.9446	20% +/- 10%	57% +/- 7%	23% +/- 13%
+ eCD4-Ig-Q40A-mim2 15 min	0.9651	41% +/- 10%	28% +/- 8%	31% +/- 12%
+ eCD4-Ig-Q40A-mim2 30 min	0.9079	29% +/- 13%	37% +/- 8%	34% +/- 20%
+ eCD4-Ig-Q40A-mim2 45 min	0.9550	14% +/- 15%	23% +/- 11%	63% +/- 20%
+ eCD4-Ig-Q40A-mim2 60 min	0.7715	6% +/- 2%	35% +/- 9%	59% +/- 13%
HIV-1$_{JR-FL}$ V4A1-R542$_{TAG}$	Curve fitting R-squared	**State 1**	**State 2**	**State 3**
		μ: 0.73+/-0.04	μ: 0.35+/-0.03	μ: 0.13+/-0.02
		σ: 0.17+/-0.03	σ: 0.10+/-0.02	σ: 0.07+/-0.01
unliganded	0.9550	63% +/- 8%	19% +/- 12%	18% +/- 9%
+ PGT151	0.9291	38% +/- 7%	44% +/- 15%	18% +/- 5%
+ sCD4$_{D1D2}$-Igαtp	0.9647	41% +/- 5%	24% +/- 5%	35% +/- 13%
+ eCD4-Ig-Q40A-mim2 15 min	0.9381	51% +/- 9%	20% +/- 15%	29% +/- 11%
+ eCD4-Ig-Q40A-mim2 30 min	0.9530	27% +/- 12%	46% +/- 23%	27% +/- 15%
+ eCD4-Ig-Q40A-mim2 45 min	0.9445	30% +/- 7%	52% +/- 26%	18% +/- 17%
+ eCD4-Ig-Q40A-mim2 60 min	0.9342	33% +/- 11%	25% +/- 9%	42% +/- 8%
HIV-1$_{NL4-3}$	Curve fitting R-squared	**State 1**	**State 2**	**State 3**
		μ: 0.1+/-0.03	μ: 0.60+/-0.05	μ: 0.30+/-0.04
		σ: 0.07+/-0.01	σ: 0.17+/-0.03	σ: 0.10+/-0.02
Unliganded	0.9857	40% +/- 11%	24% +/- 12%	36% +/- 15%
+ 17b	0.9833	21% +/- 5%	29% +/- 11%	50% +/- 10%
+ F105	0.9781	22% +/- 6%	32% +/- 12%	46% +/- 12%

The FRET histograms were carefully fitted into the sum of three Gaussian distributions with defined means and variances for each state, based on observation of original FRET signals and determined using hidden Markov modelling. μ, the mean or expectation of the Gaussian distribution; σ, s.d. of the Gaussian distribution. For FRET data obtained from different HIV-1 Env strains, or the same strains with different labelling positions or that contain or lack labelling peptides, the shapes of Gaussian distributions may vary slightly. These HIV-1 Env variants were therefore analysed and grouped separately. Relative state occupancies are presented as mean ± s.e.m., determined from three independent measurements. R^2 values were calculated to evaluate the goodness of fit.

Supplementary Material

Refer to Web version on PubMed Central for supplementary material.

Acknowledgements

We thank A. B. Ward, R. W. Sanders and P. J. Bjorkman for discussions, R. Blakemore for assistance with molecular modelling, D. Burton and M. Feinberg for reagents including PGT121, PGT122, PGT145, PGT151 and NC-Cow1, NC-Cow8, NC-Cow9 and NC-Cow10 antibodies, and the AIDS Research and the Reference Reagent Program (Division of AIDS, NIAID, NIH) for the antibodies 3BNC117, 10-1074, PG9 and PG16. This work was supported by NIH grants RO1 GM116654 and UM1 AI100645 to W.M., RO1 GM098859 to S.C.B., RO1 AI124982 and RO1 AI100645 to J.G.S., K22 AI116262 to J.B.M., CRC Tier 2 RCHS0235 and a CIHR foundation grant 352417 to A.F., PO1 GM056550 to W.M., J.G.S., S.C.B, A.B.S. and C.A., by a Brown Coxe Fellowship to M.L., a fellowship from the China Scholarship Council-Yale World Scholars to X.M., by the International AIDS Vaccine Initiative's (IAVI's) Neutralizing Antibody Consortium to P.D.K. and by the Intramural Research Program of the Vaccine Research Center (NIAID, NIH) to P.D.K. and A.B.M., and by the SFB1129 and the Emmy-Noether programme (project number 317530061) of the German Research Foundation to E.A.L. and I.N.-S., respectively.

Reviewer information *Nature* thanks David Millar, Alexandra Trkola and the other anonymous reviewer(s) for their contribution to the peer review of this work.

References

1. Harrison SC Viral membrane fusion. Nat. Struct. Mol. Biol 15, 690–698 (2008). [PubMed: 18596815]
2. Wyatt R & Sodroski J The HIV-1 envelope glycoproteins: fusogens, antigens, and immunogens. Science 280, 1884–1888 (1998). [PubMed: 9632381]
3. Kwong PD et al. Structure of an HIV gp120 envelope glycoprotein in complex with the CD4 receptor and a neutralizing human antibody. Nature 393, 648–659 (1998). [PubMed: 9641677]
4. Liu J, Bartesaghi A, Borgnia MJ, Sapiro G & Subramaniam S Molecular architecture of native HIV-1 gp120 trimers. Nature 455, 109–113 (2008). [PubMed: 18668044]
5. Ozorowski G et al. Open and closed structures reveal allostery and pliability in the HIV-1 envelope spike. Nature 547, 360–363 (2017). [PubMed: 28700571]
6. Haynes BF & Burton DR Developing an HIV vaccine. Science 355, 1129–1130 (2017). [PubMed: 28302812]
7. Sanders RW & Moore J P Native-like Env trimers as a platform for HIV-1 vaccine design. Immunol. Rev 275, 161–182 (2017). [PubMed: 28133806]
8. Munro JB et al. Conformational dynamics of single HIV-1 envelope trimers on the surface of native virions. Science 346, 759–763 (2014). [PubMed: 25298114]
9. Herschhorn A et al. Release of gp120 restraints leads to an entry-competent intermediate state of the HIV-1 envelopeglycoproteins. mBio 7, e01598–e16 (2016). [PubMed: 27795397]
10. Ma X et al. HIV-1 Env trimer opens through an asymmetric intermediate in which individual protomers adopt distinct conformations. eLife 7, e34271 (2018). [PubMed: 29561264]
11. Sanders RW et al. A next-generation cleaved, soluble HIV-1 Env trimer, BG505 SOSIP.664gp140, expresses multiple epitopes for broadly neutralizing but not non-neutralizing antibodies. PLoS Pathog. 9, e1003618 (2013). [PubMed: 24068931]
12. Julien JP et al. Crystal structure of a soluble cleaved HIV-1 envelope trimer. Science 342, 1477–1483 (2013). [PubMed: 24179159]
13. Lyumkis D et al. Cryo-EM structure of a fully glycosylated soluble cleaved HIV-1 envelope trimer. Science 342, 1484–1490 (2013). [PubMed: 24179160]
14. Pancera M et al. Structure and immune recognition of trimeric pre-fusion HIV-1 Env. Nature 514, 455–461 (2014). [PubMed: 25296255]
15. Wang H et al. Cryo-EM structure of a CD4-bound open HIV-1 envelope trimer reveals structural rearrangements of the gp120 V1V2 loop. Proc. Natl Acad. Sci. USA 113, E7151–E7158 (2016). [PubMed: 27799557]

16. Bartesaghi A, Merk A, Borgnia MJ, Milne JL & Subramaniam S Prefusion structure of trimeric HIV-1 envelope glycoprotein determined by cryo-electron microscopy. Nat. Struct. Mol. Biol 20, 1352–1357 (2013). [PubMed: 24154805]
17. Gristick HB et al. Natively glycosylated HIV-1 Env structure reveals new mode for antibody recognition of the CD4-binding site. Nat. Struct. Mol. Biol 23, 906–915 (2016). [PubMed: 27617431]
18. Kwon YD et al. Crystal structure, conformational fixation and entry-related interactions of mature ligand-free HIV-1 Env. Nat. Struct. Mol. Biol 22, 522–531 (2015). [PubMed: 26098315]
19. Lee JH, Ozorowski G & Ward AB Cryo-EM structure of a native, fully glycosylated, cleaved HIV-1 envelope trimer. Science 351, 1043–1048 (2016). [PubMed: 26941313]
20. Chuang GY et al. Structure-based design of a soluble prefusion-closed HIV-1 Env trimer with reduced CD4 affinity and improved immunogenicity. J. Virol 91, e02268–e16 (2017). [PubMed: 28275193]
21. Sakin V et al. A versatile tool for live-cell imaging and super-resolution nanoscopy studies of HIV-1 Env distribution and mobility. Cell Chem. Biol 24, 635–645 (2017). [PubMed: 28457706]
22. Sen J, Jacobs A & Caffrey M Role of the HIV gp120 conserved domain 5 in processing and viral entry. Biochemistry 47, 7788–7795 (2008). [PubMed: 18597484]
23. Alsahafi N, Debbeche O, Sodroski J & Finzi A Effects of the I559P gp41 change on the conformation and function of the human immunodeficiency virus (HIV-1) membrane envelope glycoprotein trimer. PLoS ONE 10, e0122111 (2015); correction 10, e0129405 (2015). [PubMed: 25849367]
24. Pancera M et al. Crystal structures of trimeric HIV envelope with entry inhibitors BMS-378806 and BMS-626529. Nat. Chem. Biol 13, 1115–1122 (2017). [PubMed: 28825711]
25. Caskey M et al. Viraemia suppressed in HIV-1-infected humans by broadly neutralizing antibody 3BNC117. Nature 522, 487–491 (2015). [PubMed: 25855300]
26. Caskey M et al. Antibody 10–1074 suppresses viremia in HIV-1-infected individuals. Nat. Med 23, 185–191 (2017). [PubMed: 28092665]
27. Nishimura Y et al. Early antibody therapy can induce long-lasting immunity to SHIV. Nature 543, 559–563 (2017). [PubMed: 28289286]
28. Sok D et al. Rapid elicitation of broadly neutralizing antibodies to HIV by immunization in cows. Nature 548, 108–111 (2017). [PubMed: 28726771]
29. Gardner MR et al. AAV-expressed eCD4-Ig provides durable protection from multiple SHIV challenges. Nature 519, 87–91 (2015). [PubMed: 25707797]
30. Castillo-Menendez LR, Nguyen HT & Sodroski J Conformational differences between functional human immunodeficiency virus envelope glycoprotein trimers and stabilized soluble trimers. J. Virol 93, e01709–e01718 (2019). [PubMed: 30429345]
31. Tang G et al. EMAN2: an extensible image processing suite for electron microscopy. J. Struct. Biol 157, 38–46 (2007). [PubMed: 16859925]
32. Lin CW & Ting AY Transglutaminase-catalyzed site-specific conjugation of small-molecule probes to proteins in vitro and on the surface of living cells. J. Am. Chem. Soc 128, 4542–4543 (2006). [PubMed: 16594669]
33. Yin J, Lin AJ, Golan DE & Walsh CT Site-specific protein labeling by Sfp phosphopantetheinyl transferase. Nat. Protoc 1, 280–285 (2006). [PubMed: 17406245]
34. Juette MF et al. Single-molecule imaging of non-equilibrium molecular ensembles on the millisecond timescale. Nat. Methods 13, 341–344 (2016). [PubMed: 26878382]
35. Dave R, Terry DS, Munro JB & Blanchard SC Mitigating unwanted photophysical processes for improved single-molecule fluorescence imaging. Biophys. J 96, 2371–2381 (2009). [PubMed: 19289062]
36. Aitken CE, Marshall RA & Puglisi JD An oxygen scavenging system for improvement of dye stability in single-molecule fluorescence experiments. Biophys. J 94, 1826–1835 (2008). [PubMed: 17921203]
37. McKinney SA, Joo C & Ha T Analysis of single-molecule FRET trajectories using hidden Markov modeling. Biophys. J 91, 1941–1951 (2006). [PubMed: 16766620]

38. Zhong P et al. Cell-to-cell transmission can overcome multiple donor and target cell barriers imposed on cell-free HIV. PLoS ONE 8, e53138 (2013). [PubMed: 23308151]

39. Poss M & Overbaugh J Variants from the diverse virus population identified at seroconversion of a clade A human immunodeficiency virus type 1-infected woman have distinct biological properties. J. Virol 73, 5255–5264 (1999) [PubMed: 10364271]

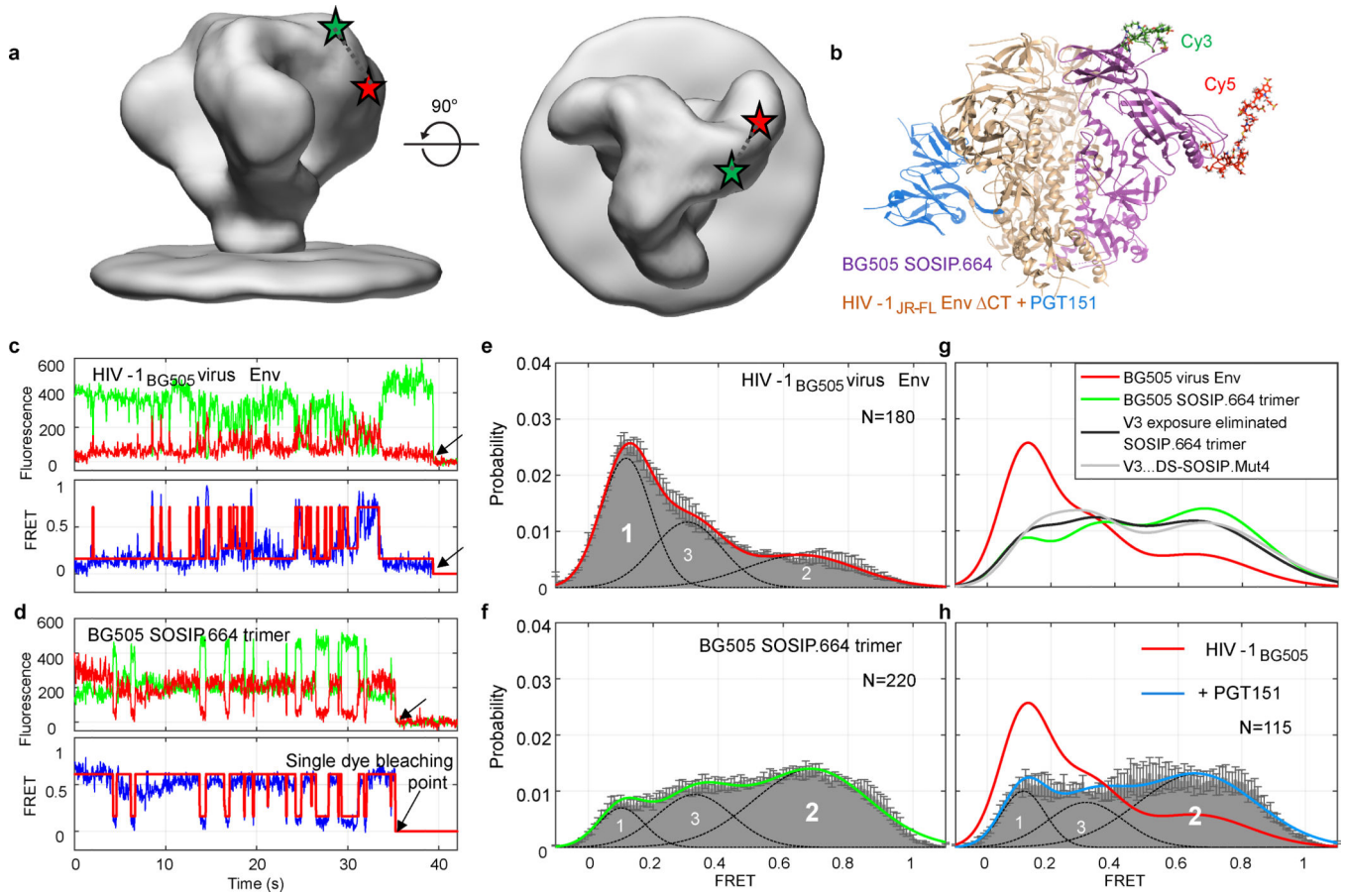

Fig. 1 |. HIV-1 Env on the surface of viruses, or in complexes characterized structurally at high resolution, reside in distinct conformational states.

a, **b**, Experimental approach. Membrane-bound HIV-1 trimer on chemically inactivated virus, depicted by cryo-electron tomography at a resolution[4] of about 20 A (left, side view; right, top view) (**a**), or Env proteins used to obtain high-resolution structures (BG505 sgp140 SOSIP.664[18] or HIV-1_{JR-FL} Env(ΔCT) in complex with PGT151[19])

(**b**) were double-labelled in a single protomer in V1 with Cy3 (green) and in V4 with Cy5 (red), and analysed by smFRET. HIV-1_{JR-FL} Env(ΔCT) in complex with PGT151[19] and unliganded BG505 sgp140 SOSIP.664[18] are adapted from RCSB Protein Data Bank accessions 5FUU (Env protomers, orange; PGT151, light blue) and 4ZMJ (magenta), respectively.

c, **d**, Example of fluorescence traces of unliganded HIV-1_{BG505} Env on the surface of an intact virus (**c**) and BG505 sgp140 SOSIP.664 (**d**) that carry fluorophores at identical positions within V1 and V4 of gp120. Top, donor Cy3 in green and acceptor Cy5 in red; bottom, resulting FRET in blue and hidden Markov model idealization in red. Arrows indicate single-step photobleaching events that define the background of our smFRET assay.

e, Unliganded HIV-1_{BG505} Env predominantly resides in state 1. FRET histogram compiled from 180 HIV-1_{BG505} Env FRET traces and fitted curve (red) for three confined Gaussian distributions (black) centred at 0.1 (low FRET, state 1), 0.33 (intermediate FRET, state 3) and 0.65 (high FRET, state 2). **f**, BG505 sgp140 SOSIP.664 predominantly samples state-2-

like conformations. Experiment as in **e**, conducted with unliganded BG505 sgp140 SOSIP.664. **g**, BG505 sgp140 SOSIP.664 variants with V3-negative selection (Extended Data Fig. 1d) retain a state 2 dominance that is similar to that of BG505 sgp140 SOSIP.664 (**f**), and all differ from the HIV-1 virus Env (**e**). **h**, Binding of PGT151 at neutralizing concentrations (10 μg ml^{-1}) stabilizes a state-2-like conformational state of HIV-1_{BG505} Env. Histograms represent mean ± s.e.m., determined from three independent populations of smFRET traces. Number of FRET traces are indicated. State occupancies and determining parameters are listed in Extended Data Table 1.

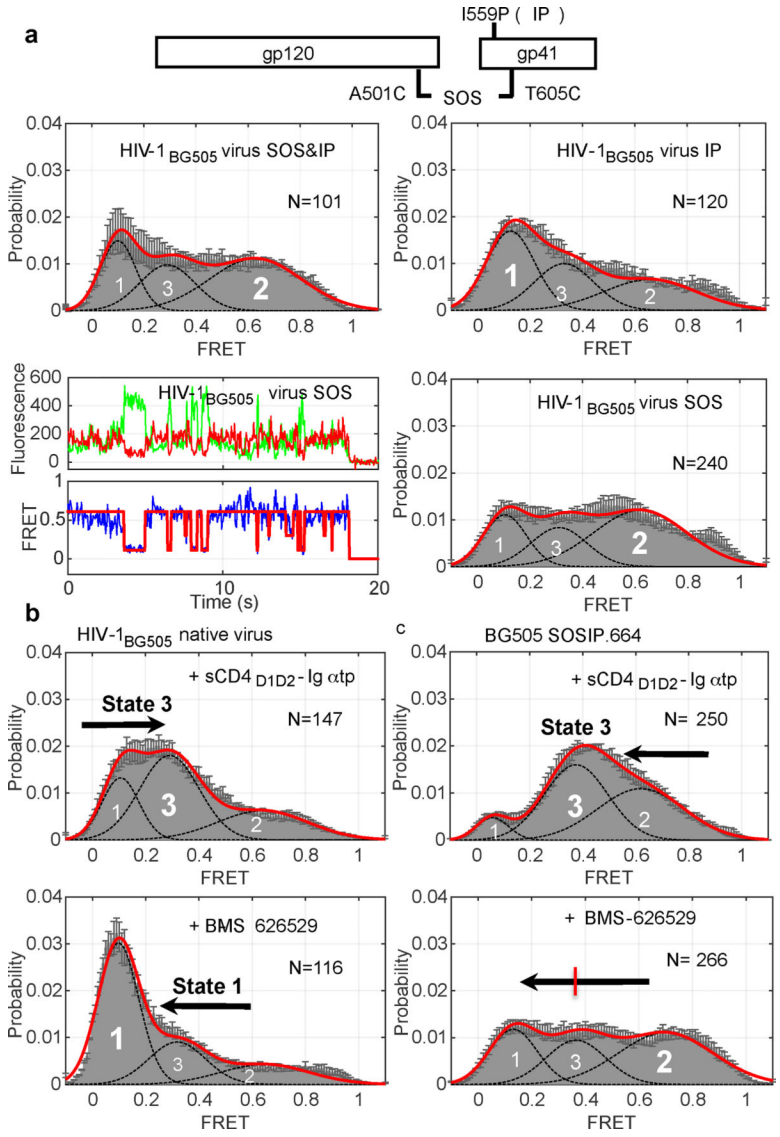

Fig. 2 |. Stabilizing disulfide bond and I559P mutations stabilize state 2.

a, The stabilizing disulfide bond is largely responsible for the stabilization of Env in state 2. Schematic shows the structure-stabilizing modifications A501C and T605C (SOS) and I559P (I559P) that were used in the design of BG505 sgp140 SOSIP.664, when introduced into HIV-1 Env on the surface of virus. FRET histograms of unliganded HIV-1_{BG505} Env carrying A501C, T605C and I559P substitutions (top left, HIV-1_{BG505} SOS and I559P), A501C and T605C substitutions (bottom right, HIV-1_{BG505} SOS; bottom left, sample trace) and I559P (top right, HIV-1_{BG505} I559P) changes, respectively. **b**, FRET histograms of HIV-1_{BG505} Env in the presence of $sCD4_{D1D2}$–Igαtp (top) and entry inhibitor BMS-626529 (bottom). **c**, Experiments as in **b**, for BG505 sgp140 SOSIP.664. FRET histograms represent mean ± s.e.m., determined from three independent groups of smFRET traces. The FRET histograms of liganded HIV-1_{BG505} Env and BG505 sgp140 SOSIP.664 in **b** and **c** can be compared with those of the unliganded Env in Fig. 1e and Fig. 1f, respectively.

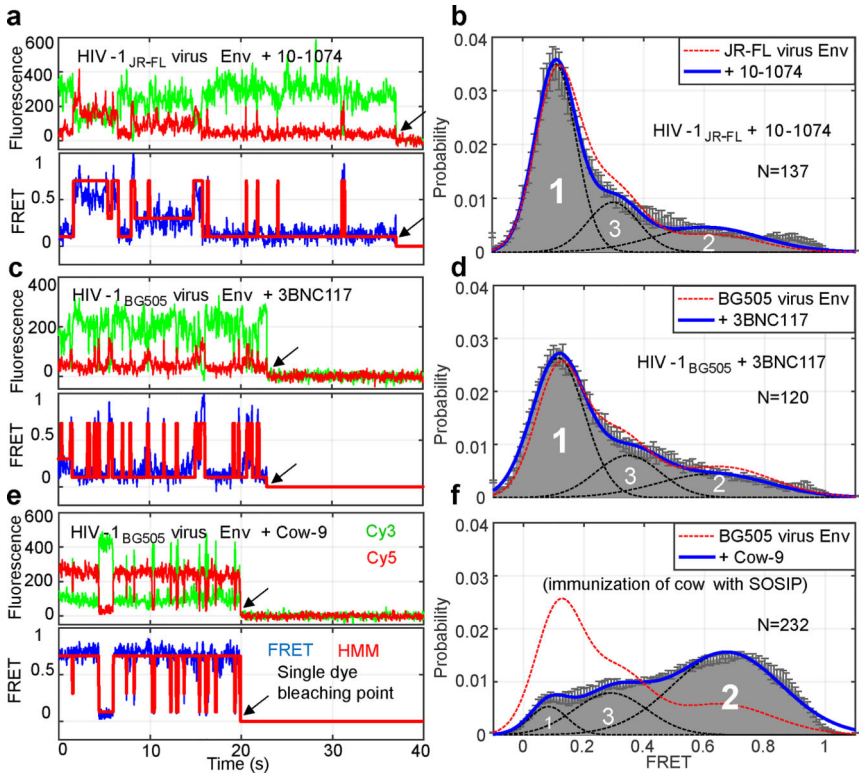

Fig. 3 |. Many broadly neutralizing antibodies exhibit a preference for state 1 of HIV-1 Env, whereas cow antibodies exhibit a preference for state 2.

a, **b**, Conformational landscape upon binding of the broadly neutralizing antibody 10–1074 (50 μg ml^{-1}) to HIV-1$_{JR-FL}$ virus Env. **a**, Sample trace (arrows defined as in Fig. 1). **b**, Histogram. FRET histogram of the unliganded HIV-1$_{JR-FL}$ virus Env is in red. **c**, **d**, Experiments as in **a**, **b**, for the broadly neutralizing antibody 3BNC117 (50 μg ml^{-1}) binding to HIV-1$_{BG505}$ Env. **e**, **f**, Sample trace (FRET in blue, hidden Markov model idealization in red) (**e**) and histogram (**f**) of NC-Cow9 antibody preference for state 2 on HIV-1 (T332N)$_{BG505}$ virus Env. This conformational profile largely resembles that of BG505 sgp140 SOSIP.664, which was used as an immunogen to elicit the NC-Cow9 antibody. FRET histograms represent mean ± s.e.m., determined from three independent populations of smFRET traces.

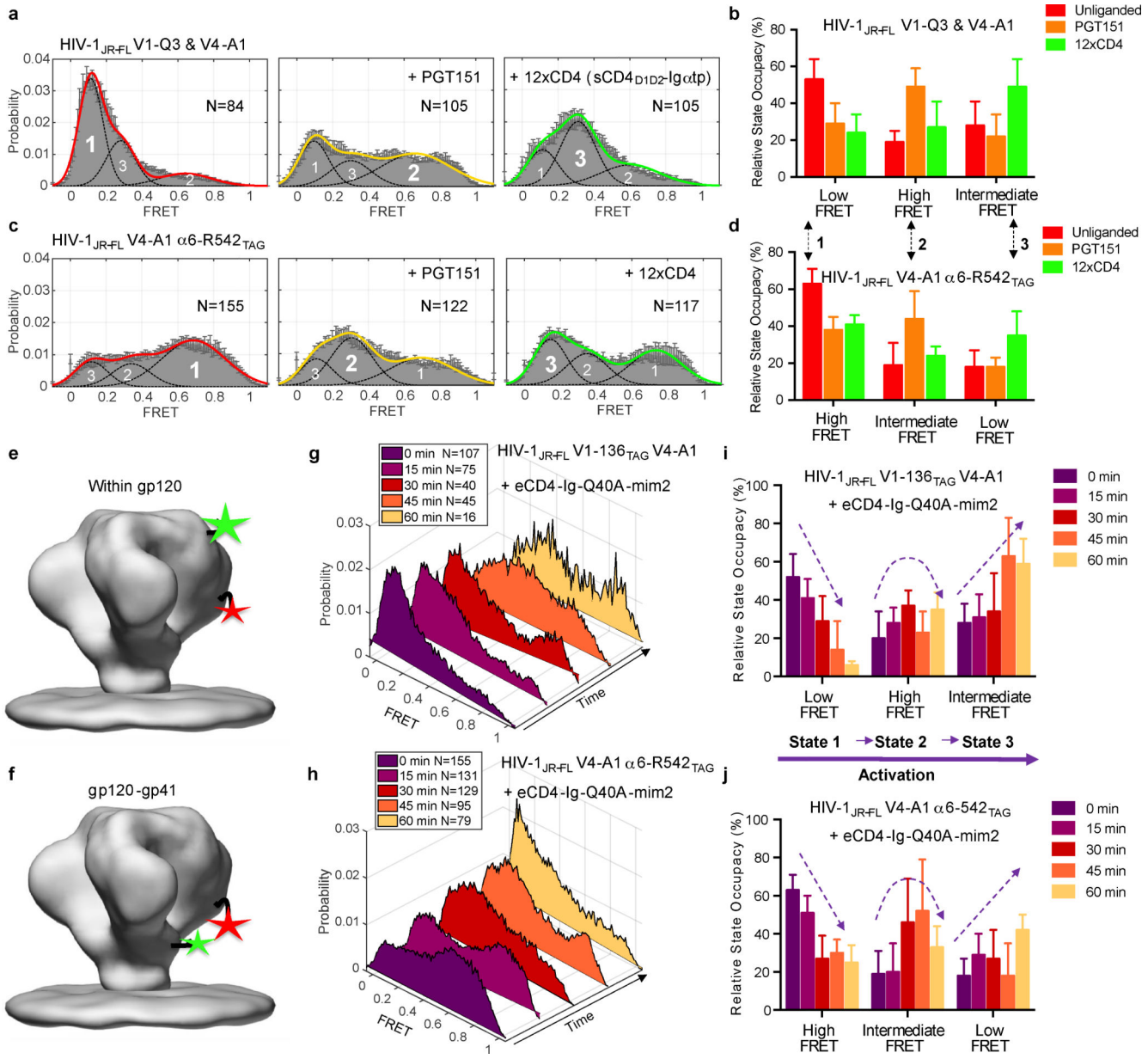

Fig. 4 |. HIV-1 Env conformational states and dynamics monitored during activation from two perspectives.

a-d, Three main conformational Env states can be observed from two perspectives. V1–Q3 and V4–A1 double-labelled HIV-1_{JR-FL} Env (**a**, **b**), and click-labelled HIV-1_{JR-FL} with fluorophores in V4 of gp120 and $Arg542_{TAG}$ in the α6 of gp41 (HIV-1_{JR-FL} V4–A1 α6–$Arg542_{TAG}$) (**c**, **d**) (see also Extended Data Fig. 9) identify preferentially occupied conformational states for the unliganded, the PGT151-bound and the 12×CD4 ($sCD4_{D1D2}$–Igαtp)-bound HIV-1_{JR-FL} Env, irrespective of the FRET values (quantified in **b** and **d**). Unliganded, PGT151-bound and $sCD4_{D1D2}$–Igαtp-bound HIV-1_{JR-FL} Env are as in Extended Data Fig. 2e, and previously reported[10]. Histograms (**a**, **c**) present mean ± s.e.m., determined from three independent populations of smFRET traces. **e–j**, Temporal progression of the Env conformational landscape, monitored from both perspectives, upon

binding of the potent bifunctional eCD4–Ig(Q40A, mim2) ligand at 100 μg ml^{-1} (Extended Data Fig. 9c). Conceptual presentation of labelling positions (**e**, **f**), three-dimensional time-resolved FRET histograms (**g**, **h**, two replicates) and relative state occupancies observed over 60 min (**i**, **j**) of click-labelled HIV-$1_{JR\text{-}FL}$ V1–Asn136_{TAG} V4–A1 and V4–A1 α6–Arg542_{TAG} upon addition of eCD4–Ig(Q40A, mim2). FRET data from 15-min intervals were combined into three-dimensional time-correlated histograms. Relative state occupancies (**b**, **d**, **i**, **j**) are presented as mean ± s.e.m., derived from histograms (**a**, **c**, **g**, **h**), respectively. The determining parameters are listed in Extended Data Table 1.